

ACCEPTED MANUSCRIPT



Negative regulation of ABA signaling by WRKY33 is critical for *Arabidopsis* immunity towards *Botrytis cinerea* 2100

Shouan Liu, Barbara Kracher, Joerg Ziegler, Rainer P Birkenbihl, Imre E Somssich

DOI: <http://dx.doi.org/10.7554/eLife.07295>

Cite as: eLife 2015;10.7554/eLife.07295

Received: 3 March 2015

Accepted: 13 June 2015

Published: 15 June 2015

This PDF is the version of the article that was accepted for publication after peer review. Fully formatted HTML, PDF, and XML versions will be made available after technical processing, editing, and proofing.

Stay current on the latest in life science and biomedical research from eLife.
[Sign up for alerts](http://elife.elifesciences.org) at elife.elifesciences.org

1 **Negative regulation of ABA signaling by WRKY33 is critical for**
2 ***Arabidopsis* immunity towards *B. cinerea* 2100**

3

4 Shouan Liu¹, Barbara Kracher¹, Joerg Ziegler², Rainer P. Birkenbihl¹ and Imre
5 E. Somssich^{1*}

6 ¹Department of Plant Microbe Interactions, Max Planck Institute for Plant
7 Breeding Research, Carl-von-Linné Weg 10, 50829 Cologne, Germany

8 ²Department of Molecular Signal Processing, Leibnitz Institute of Plant
9 Biochemistry, Weinberg 3, 06120 Halle (Saale), Germany

10

11

12

13 *Corresponding author:

14 Imre E. Somssich

15 +49-221-5062-310

16 Email: somssich@mpipz.mpg.de

17

18

19

20

21

22 **Abstract**

23 The *Arabidopsis* mutant *wrky33* is highly susceptible to *Botrytis cinerea*. We
24 identified >1680 *Botrytis*-induced WRKY33 binding sites associated with 1576
25 *Arabidopsis* genes. Transcriptional profiling defined 318 functional direct target
26 genes at 14 h post inoculation. Comparative analyses revealed that WRKY33
27 possess dual functionality acting either as a repressor or as an activator in a
28 promoter-context dependent manner. We confirmed known WRKY33 targets
29 involved in hormone signaling and phytoalexin biosynthesis, but also
30 uncovered a novel negative role of abscisic acid (ABA) in resistance towards
31 *B. cinerea* 2100. The ABA biosynthesis genes *NCED3* and *NCED5* were
32 identified as direct targets required for WRKY33-mediated resistance.
33 Loss-of-WRKY33 function resulted in elevated ABA levels and genetic studies
34 confirmed that WRKY33 acts upstream of *NCED3/NCED5* to negatively
35 regulate ABA biosynthesis. This study provides the first detailed view of the
36 genome-wide contribution of a specific plant transcription factor in modulating
37 the transcriptional network associated with plant immunity.

38

39

40 **Introduction**

41 Necrotrophic fungi including *Botrytis cinerea*, *Fusarium oxysporum*, and
42 *Alternaria brassicicola*, are the largest class of fungal phytopathogens causing
43 serious crop losses worldwide (Łażniewska *et al.*, 2010). These pathogens
44 extract nutrients from dead host cells by producing a variety of phytotoxic
45 compounds and cell wall degrading enzymes (Mengiste, 2012; Williamson *et*
46 *al.*, 2007). *B. cinerea* has a broad host-range, causes pre- and postharvest
47 disease, and is the second most agriculturally important fungal plant pathogen
48 (Dean *et al.*, 2012).

49 Plant immunity towards *B. cinerea* appears to be under complex poorly
50 understood genetic control (Rowe and Kliebenstein, 2008). Apart from the
51 *Arabidopsis thaliana* *RESISTANCE TO LEPTOSPHAERIA MACULANS 3*
52 (*RLM3*), no major *R-gene* has been associated with resistance to necrotrophs.
53 However, over the past two decades numerous genes that influence the
54 outcome of *B. cinerea* - host interactions have been identified (Mengiste,
55 2012). Among these are several transcription factors (TFs) consistent with the
56 large transcriptional reprogramming observed in host cells upon *Botrytis*
57 infection (Birkenbihl *et al.*, 2012; Birkenbihl and Somssich, 2011; Windram *et*
58 *al.*, 2012). In *Arabidopsis* several MYB-type TFs regulate distinct host
59 transcriptional responses towards *B. cinerea*. BOS1 (*BOTRYTIS*
60 *SUSCEPTIBLE 1*)/MYB108 appears to restrict necrosis triggered by *B. cinerea*

61 and *A. brassicicola*, and loss-of-BOS1 function increased plant susceptibility
62 (Mengiste, 2012). In response to stress and *B. cinerea* infection, BOS1
63 physically interacts with and is ubiquitinated by BOI, a RING E3 ligase that
64 contributes to defense by restricting the extent of necrosis (Luo *et al.*, 2010).
65 MYB51 is involved in the transcriptional activation of indole glucosinolate
66 biosynthetic genes, which also contributes to resistance towards necrotrophs
67 (Kliebenstein *et al.*, 2005; Sánchez-Vallet *et al.*, 2010). In contrast, the
68 MYB-related genes *ASYMMETRIC LEAVES 1 (AS1)* and *MYB46* appear to
69 play a role in disease susceptibility as such mutants show increased disease
70 resistance towards *B. cinerea* (Nurnberg *et al.*, 2007; Ramírez *et al.*, 2011).

71

72 Ethylene and jasmonic acid (ET, JA) signaling are critical for host immunity to
73 necrotrophic pathogens, and several transcriptional activators and repressors
74 of the ET and JA pathways impact resistance to *B. cinerea* (Bari and Jones,
75 2009; Glazebrook, 2005). In particular the TFs ERF1, ORA59, ERF5, ERF6,
76 and RAP2.2, have regulatory functions in host susceptibility to this fungus.
77 (Berrocal-Lobo *et al.*, 2002; Moffat *et al.*, 2012; Pré *et al.*, 2008; Zhao *et al.*,
78 2012). Transgenic *Arabidopsis* lines over-expressing *ERF1* or *ORA59* confer
79 resistance to *B. cinerea* (Kazan and Manners, 2013) whereas *RNAi-ORA59*
80 silenced lines were more susceptible (Berrocal-Lobo *et al.*, 2002; Pré *et al.*,
81 2008). Both ERF1 and ORA59 appear to be key integrators of the ET- and

82 JA-signaling pathways (Pieterse *et al.*, 2009). In contrast, the bHLH
83 transcription factor MYC2/JIN1 is a master regulator of diverse JA-mediated
84 responses by antagonistically regulating two distinct branches of the JA
85 signaling pathway in response to necrotrophs (Kazan and Manners, 2013).

86

87 The WRKY family of TFs modulate numerous host immune responses
88 (Pandey and Somssich, 2009). In particular, WRKY33 is a key positive
89 regulator of host defense to both *A. brassicicola* and *B. cinerea* (Birkenbihl *et*
90 *al.*, 2012; Zheng *et al.*, 2006). WRKY33 was directly phosphorylated *in vivo* by
91 the MAP kinases MPK3 and MPK6 upon *B. cinerea* infection, and
92 subsequently activated *PAD3* expression by direct binding to its promoter (Mao
93 *et al.*, 2011). *PAD3* encodes a key biosynthetic enzyme required for the
94 production of the antimicrobial compound camalexin. Moreover, WRKY33
95 directly interacted with its own promoter, suggesting a positive feedback
96 regulatory loop on *WRKY33* expression. WRKY33 was also found to interact
97 with the VQ-motif containing protein MAP KINASE SUBSTRATE1
98 (MKS1/VQ21) and to form a ternary complex with the MAP kinases MPK4
99 within the nucleus of resting cells (Andreasson *et al.*, 2005; Qiu *et al.*, 2008).
100 Upon challenge with the hemibiotrophic pathogen *Pseudomonas syringae* or
101 upon elicitation by the Microbe-Associated Molecular Pattern (MAMP) flg22,
102 the active epitope of the bacterial flagella, activated MPK4 phosphorylates

103 MKS1 thereby releasing WRKY33 from the complex and leading to its
104 detection at the *PAD3* promoter.

105

106 We previously reported that activation of *Arabidopsis* WRKY33 resulted in
107 rapid and massive host transcriptional reprogramming upon infection with *B.*
108 *cinerea* strain 2100 (Birkenbihl *et al.*, 2012). Compared to resistant wild-type
109 (WT) plants, susceptible *wrky33* mutants displayed early inappropriate
110 activation of salicylic acid (SA)-related host responses, elevated SA and JA
111 levels, and down-regulation of JA-associated responses at later infection
112 stages. Consistent with these results ChIP analysis demonstrated that
113 WRKY33 directly binds to the regulatory regions of *JAZ1* and *JAZ5*, two genes
114 encoding repressors of JA signaling, but also to the ERF class TF gene
115 *ORA59* involved in JA-ET crosstalk, and to two camalexin biosynthesis genes
116 *CYP71A13* and *PAD3* (Birkenbihl *et al.*, 2012). Although *pad3* plants are
117 susceptible to *B. cinerea* 2100, *wrky33* mutants are more highly susceptible.
118 Genetic studies revealed that altered SA responses at later infection stages
119 may contribute to the susceptibility of *wrky33* to *B. cinerea*, but were
120 insufficient for WRKY33-mediated resistance (Birkenbihl *et al.*, 2012). Thus,
121 WRKY33 apparently targets additional genes whose functions are critical for
122 establishing full WRKY33-dependent resistance towards this necrotroph.

123

124 In this paper we performed ChIP-seq and RNA-seq analyses to identify
125 WRKY33 regulated target genes in the *Arabidopsis thaliana* genome following
126 infection with *B. cinerea* 2100. The study uncovered numerous targets many of
127 which are associated with the regulation of hormonal signaling pathways.
128 Expression of the majority of WRKY33 direct targets is down-regulated upon
129 infection, but some, notably genes of camalexin biosynthesis, are strongly
130 up-regulated, indicating that WRKY33 is a dual-functional TF acting in a
131 promoter-context dependent manner. Subsequent genetic and hormonal
132 studies verified components of abscisic acid (ABA) biosynthesis as being
133 critical for WRKY33-dependent resistance towards this necrotrophic fungus.
134 This study provides the first genome-wide view of the gene regulatory network
135 underlying plant immunity governed by a host specific transcription factor.

136

137 **Results**

138 **Genome-wide detection of *Arabidopsis* WRKY33 binding sites in** 139 **response to *B. cinerea* 2100**

140 To gain a deeper insight into how WRKY33 regulates plant immunity towards
141 *B. cinerea* 2100, we performed ChIP-seq for genome-wide *in vivo* identification
142 of WRKY33 DNA-binding sites. For this, a transgenic *wrky33* null mutant
143 expressing an HA epitope-tagged WRKY33 construct under the control of its
144 native promoter ($P_{WRKY33}:WRKY33-HA$) was used. This line complemented the

145 *B. cinerea* 2100 susceptibility phenotype of *wrky33* plants resulting in
146 resistance similar to WT Col-0 plants (Birkenbihl *et al.*, 2012). Rosette leaves
147 of 4-week old plants, mock treated or spray-inoculated with spores of *B.*
148 *cinerea* 2100, were collected at 14 hours post inoculation and used to perform
149 ChIP-seq. The 14 h timepoint was selected based on the induced
150 WRKY33-HA protein levels observed in western blots (*Figure 1A*). No
151 WRKY33-HA protein was detected in the absence of infection. Besides the
152 non-induced sample, we used identically treated WT plant tissue lacking
153 *WRKY33-HA* as an additional negative control. Two biological replicates each
154 were analyzed. The previously identified WRKY33 *in vivo* target genes,
155 *CYP71A13* and *PAD3*, were used to monitor by ChIP-qPCR specific
156 enrichment in samples used for library construction and sequencing
157 (Birkenbihl *et al.*, 2012).

158 We identified 1684 high confidence WRKY33 binding sites common to both
159 replicates, which are associated with 1576 genes (*Figure 2C, Supplementary*
160 *file 1*). WRKY33 binding to all detected sites was dependent on prior infection
161 with *B. cinerea* 2100. Over 78 % of the identified peak regions were located in
162 promoter (1kb region upstream of the transcription start site) or 5' intergenic
163 regions (*Figure 1B*) and 15.4% were located near transcription termination
164 sites (TTS). Less than 1% and 5% of the peaks were located in exons and
165 intronic regions, respectively (*Figure 1B*). The genome-wide local distribution

166 of peak regions relative to genes showed clear accumulation of WRKY33
167 binding at about -300 bp from the transcription start sites (*Figure 1C*). The
168 fidelity of the ChIP-seq data was subsequently confirmed by ChIP-qPCR for a
169 number of genes (*Supplementary file 2*). Moreover, nearly all previously
170 reported WRKY33 *in vivo* targets including *PAD3*, *CYP71A13*, *ACS2*, *JAZ1*,
171 *ORA59*, *TRX-h5*, and *WRKY33* itself were successfully identified in our
172 ChIP-seq dataset (Birkenbihl *et al.*, 2012; Li *et al.*, 2012; Mao *et al.*, 2011).

173 Numerous studies have revealed that WRKY proteins specifically bind to a
174 DNA motif, TTGACT/C, termed the W-box (Rushton *et al.*, 2010), although
175 adjacent bases (W-box extended motifs) can also influence binding
176 (Ciolkowski *et al.*, 2008). Using the DREME/MEME software we determined
177 conserved consensus sequences within high confidence WRKY33 binding
178 sites across the genome. Of the 1684 identified WRKY33 binding regions, 80%
179 contained the well-established W-box motif (*Figure 1D*). We also found W-box
180 extended sequence motifs within the WRKY33 binding regions (*Figure 1 -*
181 *figure supplement 1A,B*). These W-box extended motifs also included the core
182 sequence GACTTTT (*Figure 1 - figure supplement 1C*), which was reported to
183 be bound by *Arabidopsis* WRKY70 and to be required for WRKY70-activated
184 gene expression (Machens *et al.*, 2014).

185 Apart from the W-box and W-box variants, we found one additional sequence
186 motif, T/GTTGAAT that occurs in 60% of the WRKY33 binding regions (*Figure*

187 1D). More than 48% (817 out of 1684) of WRKY33 binding peaks contained
188 both this new motif and the W-box (*Figure 1 - figure supplement 1D*). We
189 performed electrophoresis mobility shift assays (EMSA) using recombinant
190 WRKY33 protein to determine whether this newly identified DNA element is
191 bound by WRKY33. Two DNA oligonucleotide probes were synthesized whose
192 sequences were derived from two WRKY33 targets (*WAKL7*, *PROPEP3*)
193 containing either one or three copies of the motif, respectively. A previously
194 described DNA oligonucleotide containing three W-boxes (Mao *et al.*, 2011)
195 and a W-box mutated version hereof served as positive and negative controls.
196 A clear interaction (mobility shift) was observed between WRKY33 and the
197 labeled W-box probe but not with W-boxmut and the two probes harboring the
198 T/GTTGAAT motifs (M-3 and M-7; *Figure 1 - figure supplement 2*). Specificity
199 of W-box binding was confirmed in competition experiments wherein only an
200 excess of the W-box probe was able to compete for binding of the protein.
201 Thus, T/GTTGAAT does not appear to be a WRKY33 direct binding site and its
202 functionality remains unclear.

203

204 **Differential expression of WRKY33 target genes upon *B. cinerea* 2100** 205 **infection**

206 ChIP-seq studies in different organisms have revealed that the majority of
207 binding sites bound by specific TFs *in vivo* do not result in altered expression

208 levels of associated genes (Chang *et al.*, 2013; Fan *et al.*, 2014; MacQuarrie *et*
209 *al.*, 2011). To investigate the impact of WRKY33 binding on target gene
210 expression, we performed RNA-seq and examined *WRKY33*-mediated gene
211 expression changes in mock and *B. cinerea* 2100 (14 hpi) treated 4-week old
212 *wrky33* and WT plants. Three independent biological replicates were
213 generated and analyzed allowing us to identify genes with consistently altered
214 expression after inoculation. In WT plants, the expression of 6101 genes was
215 altered 2-fold or more ($P \leq 0.05$) compared to non-infected plants, with 3048
216 genes being up-regulated and 3053 genes being down-regulated (*Figure 2A*).
217 In *wrky33*, upon infection, the expression of 7441 genes was altered more than
218 2-fold, 3583 of them being up-regulated and 3858 down-regulated. A common
219 set of 4686 genes showed changes upon infection in both genotypes (*Figure*
220 *2A,B*). Comparative profiling of mock-treated plants identified 705 genes that
221 were differentially expressed between *wrky33* and WT in the absence of the
222 pathogen, 458 of them being up-regulated and 247 down-regulated (*Figure*
223 *2A*). Comparing the expression profiles of *B. cinerea*-infected *wrky33* and WT
224 plants (*wrky33 B.c* versus *WT B.c*), we identified 2765 differentially expressed
225 genes dependent on WRKY33, of which 1675 were up-regulated in the mutant
226 (termed WRKY33-repressed genes) and 1090 were down-regulated in the
227 mutant (termed WRKY33-induced genes; *Figure 2A,C*).
228 We then compared the WRKY33-dependent differentially expressed gene set

229 obtained by RNA-seq with the WRKY33 target gene set revealed by CHIP-seq.
230 This comparison identified 318 WRKY33-regulated target genes that were both
231 bound by WRKY33 and exhibited WRKY33-dependent altered gene
232 expression (*Figure 2C*). Of these, 240 (75%) were repressed upon infection
233 while 78 (25%) were induced (*Figure 2C,D*). We named those genes
234 WRKY33-repressed targets and WRKY33-induced targets, respectively.
235 Based on this analysis WRKY33 appears to have a prominent repressive role
236 on the transcription of many specific host genes indicating a negative
237 regulatory function of WRKY33 in mediating immunity to this pathogen. Genes
238 displaying altered expression in the *wrky33* mutant compared to WT but
239 showing no binding of WRKY33 at their respective gene loci were defined as
240 WRKY33-dependent non-targets (1435 WRKY33-repressed non-targets and
241 1012 WRKY33-induced non-targets; *Figure 2C*). The overlap between
242 observed WRKY33 binding and altered expression of the associated genes
243 upon fungal infection was around 20% (318 of 1576). This fraction is similar to
244 values reported for other plant transcription factors such as EIN3, HBI1 and
245 BES1 (Chang *et al.*, 2013; Fan *et al.*, 2014; Yu *et al.*, 2011).

246

247 **WRKY33 represses transcription of many plant immunity genes**

248 Compared to the entire genome the identified WRKY33-regulated targets were
249 significantly enriched in gene ontology (GO) categories involved in diverse

250 biological processes and molecular functions related to different forms of
251 stress, external and endogenous stimuli, signal transduction, transport,
252 metabolic processes and catalytic activity ($P < 0.05$; *Figure 2 - figure*
253 *supplement 1*), and many of these genes are repressed upon *B. cinerea*
254 infection (*Figure 2E*). For example, genes related to “defense response” were
255 highly overrepresented among WRKY33-repressed targets (38%) and in the
256 WRKY33-repressed non-target sets (17%), suggesting that WRKY33 mainly
257 functions as a repressor of plant defense responses. However, it is important
258 to note that nearly 18% of the WRKY33-induced targets were associated to
259 defense responses compared to only 3% of the WRKY33-induced non-targets.
260 This indicates that WRKY33 can also acts as a direct activator of defense gene
261 expression, very likely in a promoter-context dependent manner. Particularly
262 prominent among the WRKY33-induced targets are genes associated with
263 responses to the phytohormone ethylene (ET; 21%).
264 Apart from hormonal pathways discussed below, genes associated with the
265 GO terms “cell death” or related to diverse “kinase activities” were markedly
266 enriched among WRKY33-repressed targets and non-targets (*Figure 2E*). 42
267 out of 318 WRKY33-regulated targets are involved in cell death, and 38 of
268 these appear to be repressed by WRKY33 (*Supplementary file 3*). This
269 WRKY33-mediated repression may be an important feature required to
270 reinforce resistance towards the necrotroph *B. cinerea* that depends on dead

271 host tissue to complete its life cycle. Furthermore, 41 of the
272 WRKY33-regulated target genes encode for various kinases, and again the
273 majority of these genes appear to be negatively regulated by WRKY33
274 (*Supplementary file 4*). For the WRKY33-regulated target *LecRK VI.2*, a critical
275 role in resistance against hemibiotrophic *P. syringae* pv. tomato DC3000 and
276 necrotrophic *Pectobacterium carotovorum* bacteria has been demonstrated
277 (Huang *et al.*, 2014; Singh *et al.*, 2012).

278 Several TF gene families involved in defense were targeted by WRKY33. In
279 total, WRKY33 binding was found at 133 TF gene loci. Predominant among
280 these are members of the AP2/ERFs, MYBs, WRKYs, and NACs families
281 (*Figure 3A*). However, expression of only 16% (21 of 133) of these genes was
282 directly modulated in a WRKY33-dependent manner after *B. cinerea* infection
283 (complete list see *Supplementary file 5*). WRKY factors are predicted to form a
284 highly interconnected regulatory sub-network (Llorca *et al.*, 2014). Indeed, 18
285 WRKY genes were identified as direct targets of WRKY33 (*Figure 3A*).
286 However, only 7 genes, *WRKY33*, *WRKY38*, *WRKY41*, *WRK48*, *WRKY50*,
287 *WRKY53* and *WRKY55*, showed altered expression upon WRKY33 binding at
288 14 hpi (*Figure 3B-G*; *Figure 3 - figure supplement 1*, *Supplementary file 5*).
289 Binding to the *WRKY33* promoter is consistent with reports suggesting a
290 positive autoregulatory feedback loop resulting in high-level accumulation of
291 *WRKY33* in response to *B. cinerea* (Mao *et al.*, 2011). In addition,

292 WRKY33-dependent altered transcription of 18 other *WRKY* genes with no
293 detectable WRKY33 binding was observed following fungal infection,
294 indicating that these genes are indirectly regulated by WRKY33
295 (WRKY33-regulated non-targets; *Figure 3A*). WRKY33 function negatively
296 affected expression of most of these *WRKY* targets.

297

298 **WRKY33 modulates transcription of genes associated with hormonal**
299 **pathways**

300 Genes encoding components of pathways related to the key phytohormone
301 signaling molecules SA, JA, ET, and ABA were highly enriched in the
302 WRKY33-regulated gene set (*Figure 2E*). Genes involved in SA response were
303 overrepresented in WRKY33-repressed targets and non-targets (*Figure 2E*).
304 This is consistent with our previous transcriptomic profiling showing that
305 WRKY33 directly or indirectly repressed the expression of genes in SA
306 biosynthesis and SA-mediated signaling (Birkenbihl *et al.*, 2012). More than
307 80% (34 out of 42) of the SA-response targets are also associated with the GO
308 term “cell death” (*Figure 2 - figure supplement 2A*), suggesting that WRKY33
309 repression of the SA pathway is linked to modulation of host cell death
310 responses.

311

312 In contrast to SA signaling genes, genes responsive to ET were highly

313 enriched in the WRKY33-induced target dataset, among them are *ACS6*,
314 *ORA59* and *ERF5* (*Figure 2E*). *ACS6* is involved in *Botrytis*-induced ethylene
315 production and plays an important role in plant immunity (Han *et al.*, 2010; Li *et*
316 *al.*, 2012). *ORA59* and *ERF5* belong to the AP2/ERF TF family with *ORA59*
317 acting as an integrator of JA and ET signaling and as a positive regulator of
318 resistance against *B. cinerea*, while *ERF5* also regulates ET signaling and is a
319 key component of chitin-mediated immunity (Moffat *et al.*, 2012; Pré *et al.*,
320 2008). Genes responsive to JA and ABA were also overrepresented in our GO
321 term analysis, but in this case similar fractions of genes were identified among
322 WRKY33-induced targets, WRKY33-repressed targets and
323 WRKY33-repressed non-targets (*Figure 2E*). Some WRKY33-regulated
324 targets were enriched in more than one hormone response (*Figure 2 - figure*
325 *supplement 2B*), suggesting the involvement of WRKY33 in hormonal
326 co-regulation or crosstalk.

327 In conclusion, our global analysis revealed that WRKY33 influences various
328 hormonal responses upon infection with *B. cinerea* 2100, and that WRKY33
329 had both a positive and a negative functional relationship with a fraction of its
330 direct targets.

331

332 **WRKY33-dependent resistance to *B. cinerea* 2100 involves ABA**

333 Our previous genetic analyses excluded a major role of SA, JA and ET

334 signaling in WRKY33-dependent resistance towards *B. cinerea* 2100 (Birkenbihl
335 *et al.*, 2012). Here, two additional genes, *GH3.2* and *GH3.3*, encoding
336 acyl-acid-amide synthetases capable of conjugating amino acids to JA and
337 auxin were identified as being WRKY33-repressed targets (*Figure 8 – figure*
338 *Supplement 3A*). *GH3.3* controls JA homeostasis in seedlings, and *gh3.2*
339 mutants showed increased resistance to *B. cinerea* (González-Lamothe *et al.*,
340 2012; Gutierrez *et al.*, 2012). Thus, we generated *wrky33 gh3.2 gh3.3* triple
341 mutant plants but did not observe restoration of WT-like resistance towards *B.*
342 *cinerea* 2100, indicating that they are not critical for WRKY33-dependent
343 defense against this fungal strain (*Figure 8 – figure Supplement 3B*).

344 Interestingly, our global binding studies also revealed that WRKY33 binds to
345 the promoter region of *NCED3* and to the 3'UTR region of *NCED5* (*Figure*
346 *4A,D*), two major genes encoding 9-cis-epoxycarotenoid dioxygenase, a key
347 enzyme in the biosynthesis of ABA (Leng *et al.*, 2014). The precise role of ABA
348 in host defense remains enigmatic and ABA can positively or negatively impact
349 the outcome of plant-microbe interactions, depending on the pathogens'
350 lifestyle (Robert-Seilaniantz *et al.*, 2011). WRKY33 binding to both gene loci
351 was confirmed by ChIP-qPCR (*Figure 4C,F*). Transcript levels of *NCED3* and
352 *NCED5* both increased in the *wrky33* mutant upon *B. cinerea* infection
353 suggesting direct negative regulation by WRKY33 (*Figure 4B,E*). WRKY33
354 also bound to the *CYP707A3* promoter, a gene involved in ABA catabolism

355 (Leng *et al.*, 2014), but its expression decreased in the *wrky33* mutant and
356 increased in WT plants after infection indicative of positive regulation by
357 WRKY33 (*Figure 4 G-I*).

358 These results suggest that WRKY33 represses ABA levels during *B. cinerea*
359 2100 infection, and that this repressor function is an important component in
360 host resistance to this pathogen.

361

362 **Negative regulation of *NCED3* and *NCED5* by WRKY33 contributes to**
363 **resistance to *B. cinerea* 2100**

364 To clarify the involvement of ABA in WRKY33-mediated host defense to *B.*
365 *cinerea* 2100, we analyzed ABA mutants with respect to their phenotypes after
366 fungal infection. Previous reports have shown that *aba2-12* (Adie *et al.*, 2007),
367 *aba3-1* (Léon-Kloosterziel *et al.*, 1996), and *nced3 nced5* (Frey *et al.*, 2012)
368 accumulated much less ABA than WT plants. Indeed, the *aba2-12*, *aba3-1*,
369 *nced3-2*, *nced5-2*, and *nced3 nced5* mutants were nearly as resistant as WT
370 plants to *B. cinerea* 2100 (*Figure 5B; Figure 5 - figure supplement 1*). To test
371 whether WT resistance towards this necrotroph is due to WRKY33-mediated
372 repression of *NCED3* and *NCED5* expression we generated *wrky33 nced3*,
373 *wrky33 nced5* double, and *wrky33 nced3 nced5* triple mutants, and tested their
374 infection phenotypes.

375 ABA deficiency severely affects plant growth leading to stunted phenotypes, as

376 observed in *nced3 nced5*, *aba2-12* and *aba3-1* mutants. A strong reduction of
377 rosette diameter was also observed in the *wrky33 nced3 nced5* mutant under
378 short day conditions (*Figure 5A*). However, unlike the *wrky33* mutant, the
379 *wrky33 nced3 nced5* triple mutant showed clear resistance to *B. cinerea* 2100
380 similar to WT plants (*Figure 5B*). In contrast, the *wrky33 nced3* and *wrky33*
381 *nced5* double mutants were as susceptible as *wrky33* (*Figure 5 - figure*
382 *supplement 2*). Consistent with the observed resistance phenotype, qPCR
383 analysis revealed strongly reduced fungal biomass in *wrky33 nced3 nced5*
384 compared to *wrky33* plants at 3 days post infection (*Figure 5C*). This clearly
385 indicates that increased expression levels of *NCED3* and *NCED5* in the
386 *wrky33* mutant contribute to susceptibility toward *B. cinerea* 2100, and that a
387 key function of *WRKY33* in host immunity towards this pathogen is to repress
388 ABA biosynthesis.

389 Since *nced3 nced5* mutants have reduced ABA levels, we tested whether
390 exogenous application of ABA to the mutants could revert the resistant
391 phenotype. Indeed, application of ABA together with the fungal spore droplet to
392 leaves of the *wrky33 nced3 nced5* triple mutant partially rendered plants
393 susceptible to *B. cinerea* 2100 (*Figure 5D*). Similar tests on WT plants did not
394 alter host resistance (*Figure 5 - figure supplement 3*).

395 *CYP707A* mutants affecting ABA metabolism were reported to accumulate
396 more ABA than lines overexpressing ABA biosynthetic genes (Finkelstein,

397 2013). We therefore also tested the phenotypes of *cyp707a1*, *cyp707a2*, and
398 *cyp707a3* following infection. Interestingly, all of these mutants remained as
399 resistant as WT plants towards the fungus (*Figure 5 - figure supplement 4*).
400 Taken together, our genetic analysis combined with our ChIP-seq and
401 expression results strongly suggest that WRKY33-mediated control of *NCED3*
402 and *NCED5* expression plays a critical role in host resistance towards *B.*
403 *cinerea* 2100.

404

405 **WRKY33 controls hormone homeostasis in response to *B. cinerea***

406 Hormonal signaling appears to be affected in the susceptible *wrky33* mutant
407 compared with the resistant WT (*Figure 2E*), and *wrky33 nced3 nced5* triple
408 mutants restore WT-like resistance. Thus, we hypothesized that WRKY33
409 plays a critical regulatory role in hormone homeostasis. To test this we
410 measured hormonal levels in WT, *wrky33*, *nced3 nced5* and *wrky33 nced3*
411 *nced5* plants following infection with *B. cinerea* 2100 at various time points. It is
412 important to note that we have previously shown that up to 40 to 48 hpi no
413 differences in fungal biomass, hyphal expansion or other phenotypic criteria
414 were observed between resistant WT and susceptible *wrky33* plants
415 (Birkenbihl *et al.*, 2012).

416 As expected, ABA and SA levels increased strongly in susceptible *wrky33*
417 compared to resistant WT plants during fungal infection (*Figure 6A,B*).

418 However, JA and ACC (precursor of ET) levels also increased strongly in
419 *wrky33* compared to WT plants (*Figure 6 C,D*). Interestingly, the elevated SA
420 levels observed in *wrky33* appear to be a direct consequence of increased
421 ABA levels as SA levels were clearly reduced in the resistant ABA-deficient
422 *wrky33 nced3 nced5* compared to *wrky33* plants post infection. Moreover, the
423 levels of JA and ACC were also reduced in *wrky33 nced3 nced5* at later
424 infection stages. This suggests that ABA signaling exerts a positive role on the
425 biosynthesis of these other hormonal components.

426 Taken together, our data indicate that a key function of WRKY33 in *B. cinerea*
427 strain 2100 challenged WT plants is to limit ABA levels. Loss of WRKY33
428 function affects hormonal homeostasis in the plant during infection leading to
429 elevated ABA activity and subsequently resulting in altered hormone signaling.

430

431 **In *wrky33 nced3 nced5* plants, expression of many up-regulated genes in**
432 ***wrky33* is restored to WT-like levels**

433 Over 75% of WRKY33-regulated target genes showed elevated expression in
434 the susceptible *wrky33* mutant after *B. cinerea* 2100 infection (*Figure 2D*). To
435 test these genes for altered expression in resistant *wrky33 nced3 nced5* plants
436 we performed qRT-PCR analyses. The transcript levels of several highly
437 expressed SA-related genes observed in *wrky33* at 24 hpi decreased in the
438 *wrky33 nced3 nced5* plants, often returning to WT states. These included:

439 *ICS1, NPR1, NPR3, NPR4, TRX-h5* and *FMO1* (Figure 7). However, not all
440 SA-related genes were similarly affected as illustrated for *EDS1, PAD4,*
441 *NIMIN1, PR1* and *PR2*, whose expression levels remained significantly higher
442 than in WT (Figure 7). These results imply that simultaneous mutations of
443 *NCED3* and *NCED5* in the *wrky33* genotype partially impair SA biosynthesis
444 and signaling.

445 Reduced transcript levels were also observed for other genes in the *wrky33*
446 *nced3 nced5* mutant at 24 hpi such as the TF genes, *ERF1, NAC019,*
447 *NAC055, NAC061, NAC090, WRKY41, WRKY48, WRKY53* and *WRKY55,*
448 indicating a positive effect of ABA on their expression (Figure 7). In contrast,
449 expression of *WRKY38* and *WRKY50* increased in *wrky33 nced3 nced5* plants
450 to even higher levels than observed in *wrky33* (Figure 7) suggesting a negative
451 effect of ABA on these genes.

452 The *Botrytis*-induced expression of other ABA response genes including
453 *ACS2, BIR1, CDPK1, MPK11,* and *CRK36* was also restored to WT levels in
454 the *wrky33 nced3 nced5* mutant (Figure 7). Interestingly *CDPK1, MPK11,*
455 *CRK36* and *NPR3* are also responsive to SA and these genes are associated
456 with the GO term 'cell death', suggesting that ABA has a positive effect on cell
457 death responses (Figure 2 – figure supplement 2A, Supplementary files 3+4).

458 In summary, *WRKY33* suppresses the expression of many of its target genes
459 by negatively regulating ABA responses. The subset of genes showing

460 restoration of WT-like expression levels in the resistant triple mutant constitute
461 prime candidates whose functions may be causal for WRKY33-mediated
462 resistance against this necrotrophic fungus.

463

464 **Discussion**

465 Signal transduction to the nucleus and a complex gene regulatory network
466 governing the massive transcriptional reprogramming in the host upon
467 pathogen perception, drives the plant immune response. TFs are key terminal
468 components of this signaling cascade and function by activating and
469 repressing the expression of numerous defense-associated genes. The TF
470 WRKY33 plays a major role in conferring resistance of *Arabidopsis* plants to
471 the fungal necrotroph *B. cinerea*. In the present work, combined genome-wide
472 binding studies and transcriptional analyses allowed us to identify WRKY33
473 binding sites within the *Arabidopsis* genome upon fungal infection, and to
474 correlate WRKY33 binding to altered transcriptional outputs. By including
475 appropriate mutants in this study we identified components of the ABA
476 hormonal pathway that act downstream of WRKY33 to mediate host
477 resistance.

478 Such a genome-wide analysis of *in vivo* target sites for a selected TF
479 expressed under its native promoter in intact pathogen-infected plant tissue
480 has not yet been reported. Thus, in a broader perspective, this study also sets

481 the framework for establishing a comprehensive gene regulatory network
482 model of plant immunity.

483

484 The number of high-affinity WRKY33 binding sites within the genome by far
485 exceeds the number of direct WRKY33 target genes affected in their
486 transcriptional response during *B. cinerea* infection. Overall, 80% of the
487 WRKY33 targets were not significantly differentially expressed in the *wrky33*
488 mutant upon infection compared to WT. This excess number of gene loci
489 bound by a given TF but unaffected in their expression is consistent with
490 previous ChIP-seq studies although the reasons for this discrepancy remain to
491 be elucidated (MacQuarrie *et al.*, 2011). One plausible explanation may be that
492 transcriptional activation/repression at specific promoter sites is context
493 dependent, and may require, apart from WRKY33 binding, additional diverse
494 signaling inputs. For example we detected strong enrichment of WRKY33
495 within the promoters of numerous genes coding for receptors of various
496 MAMPs and Damage-Associated Molecular Patterns (DAMPs) including
497 *FLS2*, *EFR*, *CERK1*, *PEPR1*, and *PEPR2*, but no altered expression of these
498 genes in the *wrky33* mutant upon *Botrytis* infection. *WRKY33* is also strongly
499 and rapidly induced during MAMP/DAMP-triggered immunity (Lippok *et al.*,
500 2007; Yamaguchi *et al.*, 2010), and thus a regulatory function of WRKY33 at
501 these promoters may require additional signals/co-factors only triggered during

502 MAMP/DAMP signaling. Additionally, spatial and temporal differences in the
503 activation of target genes need to be considered. The current paper provides a
504 snapshot of global WRKY33 function during *Botrytis* infection. Whether
505 WRKY33 binding results in temporally distinct transcription patterns, as was
506 observed for EIN3 in the ethylene response, remains to be investigated
507 (Chang *et al.*, 2013). However, such studies employing living pathogens on
508 intact host plants remain challenging due to the asynchrony of the infection
509 process at various cellular sites within the tissue.

510 Nevertheless, using conservative criteria for selecting differentially expressed
511 genes in *wrky33* mutants compared to WT plants after *B. cinerea* 2100
512 infection, about 2600 genes were identified that showed transcriptional up- or
513 down-regulation. The strikingly high number of modulated genes at early
514 infection stages (14hpi) highlights the importance of WRKY33 to initiate host
515 responses to this pathogen.

516

517 **WRKY33 regulation of ABA signaling is critical for host defense towards**
518 ***B. cinerea***

519 The role of ABA in biotic stress responses is complex and currently ill-defined.
520 The ability of *Arabidopsis* to restrict penetration by the non-host barley
521 pathogen *Blumeria graminis* was shown to be dependent on the NAC TF
522 ATAF1-mediated repression of ABA biosynthesis (Jensen *et al.*, 2008). In

523 contrast, overexpression of *ATAF1* resulted in enhanced susceptibility of
524 *Arabidopsis* plants to *B. cinerea* (Wang *et al.*, 2009). *ATAF1* was shown to
525 directly bind to the *NCED3* promoter, which positively correlated with increased
526 *NCED3* expression and ABA levels (Jensen *et al.*, 2013). Moreover,
527 transcriptomic studies using 4-week old detached *Arabidopsis* leaves infected
528 with *B. cinerea* strain pepper revealed that genes involved in the suppression
529 of ABA accumulation and signaling were up-regulated at early infection stages
530 (Windram *et al.*, 2012). Our study clearly demonstrates that increased
531 expression of *WRKY33* target genes associated with ABA biosynthesis
532 (*NCED3* and *NCED5*) are causal for the susceptibility of *wrky33* to *B. cinerea*
533 2100, and the ABA deficient *wrky33 nced3 nced5* mutant restored WT-like
534 resistance towards this necrotroph. Hence, our findings reveal a novel role of
535 *WRKY33* in modulating host resistance to *B. cinerea* by suppressing ABA
536 accumulation/signaling (*Figure 8 – figure supplement 1*). Interestingly,
537 resistance to the necrotrophic fungus *Plectosphaerella cucumerina* is also
538 negatively impacted by ABA, and *wrky33-1* mutant plants exhibited an
539 enhanced susceptible phenotype towards this pathogen (Sánchez-Vallet *et al.*,
540 2012). Stimulating *NCED3* expression and ABA biosynthesis has also been
541 described as an important virulence strategy employed by the hemi-biotroph
542 *Pseudomonas syringae* DC3000 in *Arabidopsis* (de Torres - Zabala *et al.*,
543 2007). Virulence to this pathogen is strongly reduced in ABA mutants. Whether

544 WRKY33 is involved in modulating ABA signaling during this host–bacterial
545 interaction, and whether *P. syringae* DC3000 suppresses *WRKY33* expression
546 is unknown.

547

548 In our experiments the expression of several NAC TF genes associated with
549 ABA regulation was affected upon *Botrytis* infection in a *WRKY33*-dependent
550 manner. In particular, increased expression of *NAC002* (*ATAF1*), *NAC019*,
551 *NAC055*, *NAC061*, *NAC068* (*NTM1*) and *NAC090* was observed in the *wrky33*
552 mutant. Like *ATAF1*, transgenic *Arabidopsis* lines overexpressing *NAC019* or
553 *NAC055* displayed enhanced susceptibility to *B. cinerea* (Bu *et al.*, 2008). In
554 contrast, the *nac019 nac055* double mutant showed increased resistance to *B.*
555 *cinerea* compared with WT plants. ABA has been shown to induce *NAC019*
556 and *NAC055* expression (Jiang *et al.*, 2009; Zheng *et al.*, 2012). Whether any
557 of these NAC factors, apart from *ATAF1*, can also target the *NCED* genes and
558 thereby enhance ABA biosynthesis in the *wrky33* mutant remains to be tested.

559

560 ABA can repress SA-, ET-, and JA/ET-dependent signaling but also positively
561 affect some JA responses (Asselbergh *et al.*, 2008; Ton *et al.*, 2009). Our
562 genetic and phytohormone studies showed that elevated ABA levels in the
563 susceptible *wrky33* mutant resulted in concomitant increases in SA, JA, and
564 ACC levels upon *B. cinerea* 2100 infection, implying a positive effect of ABA on

565 these hormone signaling components. Increased SA levels per se in the
566 *wrky33* mutant however do not contribute to susceptibility as *wrky33 sid2*
567 double mutant plants are as susceptible to *B. cinerea* 2100 as the single
568 mutant (Birkenbihl *et al.*, 2012; *Figure 8 - figure supplement 1*). Interestingly
569 concurrent increases in ABA, JA/ET and SA have also been observed in the
570 interaction of *Arabidopsis* with *P. syringae* DC3000 and with the vascular
571 oomycete pathogen *Pythium irregular* (Adie *et al.*, 2007; de Torres - Zabala *et*
572 *al.*, 2007). In the case of *P. irregular* however, host resistance correlated with
573 high ABA levels whereas ABA mutants were clearly more susceptible.

574 Our molecular analysis of *Botrytis*-challenged *wrky33* and *wrky33 nced3*
575 *nced5* plants confirmed that elevated ABA levels mainly activate
576 NPR1-dependent SA signaling while not affecting the upstream EDS1-PAD4
577 pathway (*Figure 7*). Increased ABA also activated *ACS2*, *ACS6*, *ERF1* and
578 *ORA59*, targets involved in ET/JA signaling. In the *wrky33 nced3 nced5* mutant
579 as in WT plants expression of *ACS6*, *ORA59*, but also *ERF5* and *PDF1.2* (data
580 not shown) was significantly reduced. However, as both genotypes are
581 resistant to *B. cinerea* these ET/JA components appear not to be essential in
582 maintaining plant resistance.

583

584 How elevated ABA levels trigger activation of these hormone signaling
585 cascades and specific TFs remains to be elucidated. The receptors for ABA

586 are known (Miyakawa *et al.*, 2013), but the molecular mechanisms linking
587 downstream ABA signaling to the other hormonal pathways requires further
588 investigation. It is conceivable that the increased ABA levels in *wrky33* during
589 *Botrytis* infection trigger the activation of currently unidentified downstream
590 ABA-response factors that bind to the ABA response elements (ABRE,
591 ACGTGG/T) or G-boxes (CACGTG) present in some gene promoters,
592 resulting in transcriptional activation. Indeed, several genes including *NAC019*,
593 *NAC061*, *FMO1*, *GH3.2* and *GH3.3* contain such conserved motifs, which
594 could respond to and be activated by ABA. In addition, the elevated levels of
595 SA in *wrky33* during *Botrytis* infection may in part be responsible for the strong
596 expression of the glutaredoxin gene *GRX480/ROXY19* observed in this mutant
597 (RNA-seq data in this study; Birkenbihl *et al.*, 2012). GRX480 binds to class II
598 TGA factors, thereby activating TGA-regulated SA responses while preventing
599 their participation in JA mediated signaling (Zander *et al.*, 2014). Plants
600 ectopically overexpressing *GRX480* are susceptible to *B. cinerea* 2100
601 (Birkenbihl *et al.*, 2012).

602

603 **WRKY33 is a dual functional transcription factor**

604 In animals and humans, several TFs can act either as transcriptional activators
605 or repressors, depending on DNA binding sequences or interaction with
606 additional co-factors (Alexandre and Vincent, 2003; Berger and Dubreucq,

607 2012; Sakabe *et al.*, 2012; Zhu *et al.*, 2012). Moreover, many human TFs
608 function as repressors as often as they act as activators (Cusanovich *et al.*,
609 2014). In plants, few factors with dual functions have been unequivocally
610 characterized. In tomato, the transcriptional activator Pti4 can repress the
611 expression of *PR10-a* by forming a complex with the SEBP repressor
612 (Gonzalez-Lamothe *et al.*, 2008). In *Arabidopsis*, the TF WUSCHEL (WUS)
613 acts mainly as a repressor in stem cell regulation, but can function as an
614 activator of *AGAMOUS(AG)* during floral patterning (Ikeda *et al.*, 2009). Also
615 WRKY proteins can act as activators or repressors, and selected family
616 members in diverse plant species have been identified as key regulators in
617 diverse plant processes (Rushton *et al.*, 2010). WRKY53 can activate or
618 repress the expression of genes, depending on the nature of the target
619 promoter sequence (Miao *et al.*, 2004). *WRKY6* activates *PR1* expression
620 while suppressing the expression of its own gene, and that of its closely related
621 family member *WRKY42* (Robatzek and Somssich, 2002). Our data show that
622 also *WRKY33* is a bi-functional TF that can act as an activator or as a
623 repressor in a promoter-context dependent manner (*Figure 8*). *WRKY33*
624 positively regulates genes involved in camalexin biosynthesis such as
625 *CYP71A13* and *PAD3* by directly binding to their promoter regions (Birkenbihl
626 *et al.*, 2012; Mao *et al.*, 2011). Our study confirmed these observations and
627 identified two additional camalexin biosynthetic genes, *AMT1* and *CYP71A12*

628 that are positively and directly regulated by WRKY33 (*Figure 8 – figure*
629 *supplement 2; Supplementary file 2*). Mutants of *CYP71A13* and *PAD3* are
630 susceptible to the necrotrophs *A. brassicicola* and *B. cinerea* (Nafisi *et al.*,
631 2007; Zhou *et al.*, 1999). Beyond this, several *Botrytis*-induced ET response
632 genes were targeted and positively regulated by WRKY33 (*Figure 2E*). Still,
633 WRKY33 had a negative regulatory relationship on the expression of >75% of
634 all targets implying that it mainly acts as a direct repressor of many defense
635 genes following pathogen challenge.

636 How WRKY33 exerts its dual regulatory functions mechanistically requires
637 further research. The simplest hypothesis would be that WRKY33 is recruited
638 to distinct repressor and activator complexes at defined promoter sites. For
639 instance, several WRKY33-interacting proteins containing a VQ motif have
640 been discovered that influence defense gene expression (Cheng *et al.*, 2012;
641 Lai *et al.*, 2011; Pecher *et al.*, 2014). VQ proteins appear to act as suppressors
642 of defense-related genes via their interaction with WRKY factors. Indeed, the
643 protein VQ4/MVQ1 appears to function as a negative regulator of WRKY-type
644 transcriptional activators including WRKY33. In a transient *Arabidopsis*
645 protoplast assay, stimulation by MAMPs resulted in degradation of VQ4/MVQ1
646 following MAPK-mediated phosphorylation enabling WRKY33 to activate
647 transcription of a defense-related reporter gene (Pecher *et al.*, 2014). Two
648 other proteins, SIB1 and SIB2, have been reported to interact with WRKY33

649 via their VQ motifs. This interaction was required to stimulate WRKY33 DNA
650 binding activity and very likely to positively regulate WRKY33-mediated
651 resistance to necrotrophic fungi (Lai *et al.*, 2011).

652 Interestingly, four VQ protein genes (*VQ8*, *VQ22/JAV1*, *VQ28*, *VQ33*) are also
653 direct targets for WRKY33 and show altered expression upon *Botrytis* infection
654 in *wrky33* compared to WT. *VQ22/JAV1* functions as a negative regulator of
655 JA-mediated defenses, and transgenic *VQ22/JAV1* RNAi lines showed
656 enhanced resistance to *B. cinerea* (Hu *et al.*, 2013). Thus, elevated levels of
657 these VQ proteins in *wrky33* may contribute to the suppression of JA signaling
658 and susceptibility to this fungus.

659 Finally, many members of the WRKY TF gene family, including *WRKY33* itself,
660 are also targets of WRKY33. The majority of *WRKY* genes are transcriptionally
661 activated during immune signaling (Pandey and Somssich, 2009).
662 Experimental and bioinformatics analyses have revealed that WRKY factors
663 form a complex and highly interconnected regulatory sub-network that is
664 positively and negatively affected by auto- and cross-regulation by various
665 WRKY factors. This WRKY web appears to be deeply interconnected to
666 various hormonal pathways at multiple levels, probably to ensure rapid and
667 efficient signal amplification while allowing for tighter control in limiting the
668 extent of the host immune response (Eulgem, 2006; Llorca *et al.*, 2014).

669

670 In summary, genome-wide binding analysis and transcriptional profiling have
671 identified potential targets of WRKY33, a key transcription factor involved in
672 mediating resistance towards the necrotroph *B. cinerea* 2100. This study
673 revealed that genes involved in ABA biosynthesis and directly regulated by
674 WRKY33 act at crucial nodes in this signaling cascade. Due to the complexity
675 of the highly interconnected hormonal signaling networks targeted by WRKY33
676 the precise molecular mechanisms underlying this resistance remain to be fully
677 elucidated. In this respect global transcriptional profiling of infected *wrky33*
678 *nced3 nced5* plants should prove extremely valuable to further narrow down
679 key genes and sub-signaling pathways required to re-establish WT-like levels
680 of resistance in this mutant.

681

682 **Materials and methods**

683 **Plant material and growth conditions**

684 For all experiments *Arabidopsis thaliana* ecotype Columbia (Col-0) was used.
685 Besides wild-type (WT), the following genotypes were employed: *wrky33*
686 (GABI_324B11), *nced3-2*, *nced5-2*, *nced3 nced5*, *aba2-12*, *aba3-1*,
687 *cyp707a1-1*, *cyp707a2-1*, *cyp707a3-1*, *wrky33 sid2-1*, *wrky33 npr1-1*, *wrky33*
688 *wrky70*, *gh3.2*, *gh3.3-1*. The double or triple mutants; *wrky33 nced3*, *wrky33*
689 *nced5*, *wrky33 nced3 nced5*, *gh3.2 gh3.3-1* and *wrky33 gh3.2 gh3.3* were
690 generated by crossing single or double mutants followed by PCR-based

691 verification using appropriate primers (*Supplementary file 6*).
692 Plants were grown for 4 weeks under short-day conditions in closed cabinets
693 (Schneijder chambers: 16 h light/ 8 h dark cycle at 22-24°C, 60% relative
694 humidity) on 42mm Jiffy-7 pots (Jiffy) to prevent contaminations from garden
695 soil. Before sewing, the Jiffy pot peat pellets were re-hydrated in water
696 containing 0.1% liquid fertilizer Wuxal (Manna).

697

698 **Pathogen inoculation procedure**

699 *B. cinerea* strain 2100 was cultivated on potato dextrose plates at 22°C for 10
700 days. Spores were collected, washed, and frozen at -80°C in 0.8% NaCl at a
701 concentration of 10^7 spores mL⁻¹. For inoculation of *Arabidopsis* plants the
702 spores were diluted in Vogel buffer prepared as previously described
703 (Birkenbihl *et al.*, 2012). For droplet inoculations, 2 µl of 2.5×10^5 spores mL⁻¹
704 were applied to single leaves of 4-week old intact plants. Leaves were excised
705 from plants only for photographic documentation. The same spore
706 concentration was used for spray inoculations of 4-week old intact plants. For
707 mock treatment, Vogel buffer was used. Plants were kept prior to and during
708 infection under sealed hoods at high humidity.

709

710 **ChIP-seq assay**

711 4-week old WT plants or plants expressing *WRKY33-HA* from the native

712 *WRKY33* promoter ($P_{WRKY33}:WRKY33-HA$) were spray inoculated or mock
713 treated for 14 h. ChIP assays were performed as previously described
714 (Birkenbihl *et al.*, 2012) following the modified protocol by Gendrel *et al.*
715 (Gendrel *et al.*, 2005), using rabbit polyclonal antibodies to HA (Sigma). ChIP
716 DNA was purified using a QIA quick PCR Purification kit (Qiagen) and
717 subjected to a linear DNA amplification (LinDA) protocol (Shankaranarayanan
718 *et al.*, 2011) which included two rounds of ‘*in vitro* transcription’ by T7 RNA
719 polymerase. The resulting LinDA DNA was used to generate sequencing
720 libraries bearing barcodes using a NEBNext ChIP-Seq Library Pre Reagent
721 Set for Illumina kit (New England Biolabs). Sequencing was performed on
722 Illumina HiSeq2500 at the Max Planck Genome Centre Cologne and resulted
723 in about 10 million 100bp single-end reads per sample. ChIP-qPCR validation
724 of *WRKY33* target genes was performed using gene specific primers
725 (*Supplementary file 7*).

726

727 **ChIP-seq data analysis**

728 Before mapping, remaining LinDA adapters and low quality sequences were
729 removed from the sequencing data using a two-step procedure. In this
730 procedure, first Bpm and t7-Bpm sites were trimmed from the 5’ end using
731 cutadapt (version 1.2.1) (Martin, 2011) with options $-e$ 0.2, $-n$ 2 and $-m$ 36
732 (otherwise default settings were used), and subsequently poly-A and poly-T

733 tails and low quality ends were trimmed and reads with overall low quality or
734 with less than 36 bases remaining after trimming were removed using
735 PRINSEQ lite (version 0.20.2) (Schmieder and Edwards, 2011) with options
736 `-trim_qual_right/left 20, trim_tail_right/left 3 -min_len 36, -min_qual_mean 25`.
737 After this pre-processing steps, the remaining high quality reads were mapped
738 to the *Arabidopsis thaliana* reference genome TAIR10
739 (<http://www.arabidopsis.org>) using Bowtie (version 0.12.7) (Langmead *et al.*,
740 2009) with options `-best -m 1` to extract only uniquely mapped reads and
741 allowing two mismatches in the first mapping steps (default settings). The
742 ChIP-seq datasets used in this study have been deposited at the GEO
743 repository (GSE66289).
744 To identify genomic DNA regions enriched in sequencing reads in the ChIP
745 sample compared to input control as well as in inoculated compared to mock
746 treated samples ('peak regions'), the peak calling algorithm of the QuEST
747 program (version 2.4) (Valouev *et al.*, 2008) was applied using the transcription
748 factor mode (option "2"), with permissive parameter settings for the peak
749 calling (option "3"). Each of the two biological replicates was first analyzed
750 separately and additionally, to obtain more exact peak locations for the
751 consistent peaks, the mapped reads of the two replicates were pooled and
752 peaks were also called for the pooled samples. To annotate the peak location
753 with respect to annotated gene features in TAIR10 the `annotatePeaks.pl`

754 function from the Homer suite (Heinz *et al.*, 2010) was used with default
755 settings. To extract consistent peaks between the replicates, a custom R
756 (<http://www.r-project.org>) function (*Source code 1*) was used that identified
757 overlapping peak regions between the replicates. Two peak regions were
758 counted as overlapping, if they overlapped by at least 50% of the smaller
759 region and a peak region was counted as consistent, if it was found to be
760 overlapping between the two individual replicates as well as the pooled
761 sample.

762 To search for conserved binding motifs in the consistent WRKY33 binding
763 regions, for each consistent peak the 500 bp sequence surrounding the peak
764 maximum was extracted and submitted to the online version of MEME-ChIP
765 (Machanick and Bailey, 2011). MEME-Chip was run with default settings, but a
766 custom background model derived from the *Arabidopsis* genome was provided
767 and “Any number of repetitions” of a motif was allowed. For visualization,
768 prominent motifs identified within MEME-ChIP by either MEME or DREME
769 were chosen. To extract the number/percentage of peak regions that contain a
770 certain motif, the online version of FIMO (Grant *et al.*, 2011) was run with the
771 peak sequences and the motif of interest (MEME/DREME output) as input and
772 a p-value threshold of 0.001.

773

774 **RNA-seq assay**

775 Total RNA was extracted from mock treated (14 hpi) and *B. cinerea* infected
776 (14 hpi) 4-week old plants (WT and *wrky33*) with using the RNeasy Plant Mini
777 (Qiagen) according to the manufacturer's instructions, and mRNA sequencing
778 libraries were constructed with barcodes using the TrueSeq RNA Sample
779 Preparation Kit (Illumina). Three biological replicates were sequenced on
780 Illumina HiSeq2500 by the Max Planck Genome Centre Cologne, resulting in
781 25-45 million 100 bp single end reads per sample. Total reads were mapped to
782 the *Arabidopsis* genome (TAIR10) under consideration of exon-intron
783 structures using the splice-aware read aligner TopHat (version 2.0.10) (Kim *et*
784 *al.*, 2013) with settings `-a 10 -g 10` and known splice sites provided based on
785 TAIR10 gene annotations. The RNA-seq datasets used in this study have been
786 deposited at the GEO repository (GSE66290).

787

788 **Statistical Analysis of RNA-seq**

789 The mapped RNA-seq reads were transformed into a count per gene using the
790 function `coverageBed` of the `bedTools` suite (Quinlan and Hall, 2010) with
791 option `-split` to consider exon-intron structures. Genes with less than 50 reads
792 in all samples together were discarded, and subsequently the count data of the
793 remaining genes was TMM-normalized and `log2`-transformed using functions
794 `'calcNormFactors'` (R package `EdgeR`) (Robinson *et al.*, 2010) and `'voom'` (R
795 package `limma`) (Law *et al.*, 2014). To analyze differential gene expression

796 between genotypes (WT, *wrky33*) and treatments (mock treated, *B. cinerea*
797 infected), we fitted a linear model with the explanatory variable
798 “genotype_treatment” (i.e. including both genotype and treatment) using the
799 function `lmFit` (R package `limma`). Subsequently, we performed moderated
800 t-tests over the four contrasts of interest. Two contrasts compare *B. cinerea*
801 infected vs mock treated samples within each genotype and the other two
802 contrasts compare *wrky33* vs. WT Col-0 plants within each treatment. In all
803 cases, the resulting P values were adjusted for false discoveries due to
804 multiple hypothesis testing via the Benjamini–Hochberg procedure. For each
805 contrast, we extracted a set of significantly differentially expressed genes
806 between the tested conditions (adj. p value < 0.05, $|\log_2FC| \geq 1$).

807

808 **Gene Ontology analysis**

809 GO term enrichment analysis on the gene sets of interest was performed using
810 the R package `goseq` (Young *et al.*, 2010) with custom GO term mappings
811 obtained from `org.At.tairGO2ALLTAIRS` within the R package (version 3.0.0)
812 `org.At.tair.db`: Genome wide annotation for Arabidopsis (Carlson, 2010). To
813 identify enriched GO terms, the Wallenius distribution was used to
814 approximate the null distribution and a probability weighting function was
815 applied to correct for potential count biases in the analyzed gene sets. The
816 resulting p values were adjusted for false discoveries due to multiple

817 hypothesis testing via the Benjamini-Hochberg procedure and for each subset
818 the significantly over-represented GO terms were extracted (adj. p value
819 <0.05). For the set of all WRKY33-regulated targets, the R package (version
820 2.18.0) topGO: Enrichment analysis for Gene Ontology (Alexa &
821 Rahnenführer, 2010) was used to visualize the GO sub-graphs induced by the
822 ten most significantly enriched GO terms in the category 'Biological Process'
823 and the five most significantly enriched GO terms in the category 'Molecular
824 Function', respectively.

825

826 **qRT-PCR**

827 Total RNA was isolated from leaves at 8, 14, 24, and 48 hpi with *B. cinerea*
828 spores as described above and reverse transcribed with oligo(dT) primer to
829 produce cDNA using the SuperScript First-Strand System for
830 Reverse-Transcription PCR following the manufacturer's protocol (Invitrogen).
831 cDNAs corresponding to 2.5 ng of total RNA was subjected to qPCR with
832 gene-specific primers (*Supplementary file 8*) using the SYBR Green reagent
833 (Bio-Rad). The qPCRs were performed on the iQ5 Multicolor Real-Time PCR
834 Detection System (Bio-Rad) with three biological replicates. The relative
835 expression was normalized to At4g26410 that was described as being highly
836 constant under varying stress conditions (Czechowski *et al.*, 2005). Data
837 shown are means \pm SD from the three biological replicates.

838

839 **Phytohormone measurements and quantification**

840 Sample processing, data acquisition, instrumental setup, and calculations

841 were performed as described (Ziegler *et al.*, 2014). Instrument specific

842 parameters for the detection of SA are shown in the Table below.

843 (3,4,5,6-D₄)-SA was obtained from Campro Scientific (Veenendal, The

844 Netherlands) and used as internal standard for SA quantification (1.5 ng per

845 sample).

MS parameters for MRM-transition of salicylic acids (SA)

Hormone	MRM transitions	Decustering potential (DP), V	Entrance potential (EP), V	Cell entrance potential (CEP), V	Collision potential (CE), V	Cell exit potential (CEX), V
SA	137 → 93	-25	-5.5	-14	-22	0
	<i>137</i> → <i>65</i>	-25	-5.5	-14	-44	0
SA-D ₄	141 → 97	-25	-5.5	-14	-22	0

Quantifier and qualifier transitions are indicated in bold and italics, respectively.

846

847 **Quantification of fungal growth by qPCR**

848 Quantification of fungal biomass relative to plant biomass by qPCR was

849 basically performed as previously described (Gachon and Saindrenan, 2004).

850 Leaves of the indicated *Arabidopsis* lines were inoculated with two 2 μl

851 droplets of *B. cinerea* spores and DNA extracted 3 days later from whole

852 leaves of similar fresh weight. The relative amounts of *B. cinerea* and

853 *Arabidopsis* DNA were determined by qPCR employing specific primers for

854 cutinase A and SKII, respectively.

855

856 **Expression of recombinant WRKY33 protein and EMSA**

857 Full-length WRKY33 protein fused with NusA and an 8xHis-tag was expressed
858 in the vector pMCSG48 in the *E. coli* strain BL21 (DE3) Magic (kindly provided
859 by Dr. Michal Sikorski and Marta Grzechowiak, Institute of Bioorganic
860 Chemistry, Poznan, Poland). Bacteria containing the *WRKY33* expression
861 construct or the empty vector were induced with 0,5 mM
862 isopropylthio- β -galactisude for 3 h at 18° C. The His-tagged protein was
863 purified using nickel affinity columns (QIAexpress Ni_NTA Fast Start, Qiagen,
864 Germany) following the instructions of the manufacturer, and subsequently
865 dialyzed against 20 mM Tris-HCl, pH 7,5 overnight at 4° C.

866 The following DNA oligonucleotides probes were synthesized and biotin
867 labeled by Sigma-Aldrich (Germany): W-box probe,

868 5'-CGTTGACCGTTGACCGAGTTGACTTTTTTA-3'; W-boxmut,

869 5'-CGTTGAACGTTGAACGAGTTGAATTTTTTA-3'; M-3,

870 5'-AATTTGAATAATCAAAGATCTTCCTTTGAATTACCTATTCAACAT-3'

871 (derived from the *PROPEP3* promoter sequence); and M-7,

872 5'-GTCCACGCTTGTTTGAATTTTCAGCCTTTGCAGGCAAGGT-3' (derived

873 from the *WAKL7* promoter sequence). Two complementary strands of the

874 oligonucleotides were annealed by heating probes to 95°C for 3 min and then

875 allowing probes to cool to room temperature overnight. Freshly prepared
876 recombinant WRKY33 protein (1µg) was incubated with the DNA probe (20
877 fmol) for 20 min at room temperature using the LightShift Chemiluminescent
878 EMSA kit (Thermo Fisher) in the presence or absence of unlabeled competitor
879 DNA. The resulting protein-DNA complexes were electrophoresed on 5% (w/v)
880 polyacrylamide gels, and then transferred to N⁺ nylon membranes in 0,5%
881 Trisborate/EDTA buffer at 380mA at 4° C for 60 min. Biotin labeled DNA
882 detection was done according to the instructions of the manufacturer (Thermo
883 Fisher). Bands were visualized using the BioRAD ChemiDoc™ MP Imaging
884 System.

885

886 **Acknowledgements**

887 We thank Dr. Annie Marion-Poll (INRA, Versailles, France) for providing seeds
888 of the *nced3*, *nced5*, and *nced3 nced5* mutants, Dr. Catherine Bellini (Umeå
889 University, Sweden) for the *gh3.3* seeds, Dr. Kamal Bouarab (Université de
890 Sherbrooke, Canada) for the *gh3.2* seeds, and Dr. Wim Soppe (MPIPZ,
891 Germany) for the *cyp707a1-1*, *cyp707a2-1*, *cyp707a3-1* seeds. The *E. coli*
892 BL21 (DE3) Magic strain harboring the expression vector pMCSG48
893 containing the WRKY33 construct was kindly provided by Dr. Michal Sikorski
894 and Marta Grzechowiak (Institute of Bioorganic Chemistry, Poznan, Poland)
895 We are grateful to Drs. Paul Schulze-Lefert and Kenichi Tsuda (MPIPZ,

896 Germany) for valuable comments and critical reading of the manuscript, and
897 Elke Logemann for excellent technical assistance. This work was partly
898 supported by an IMPRS PhD fellowship (S.L.) and by the Deutsche
899 Forschungsgemeinschaft (DFG) grant SFB670 (I.E.S.).

900

901 **Competing interest**

902 The authors declare that no competing interests exist.

903

904 **Figure Legends**

905 **Figure 1.** Genome-wide identification of *Arabidopsis* WRKY33 binding sites.

906 (A) Western-blot analysis of WRKY33-HA protein levels after mock treatment

907 or spray-inoculation of $P_{WRKY33}:WRKY33-HA$ transgenic plants with *B. cinerea*

908 2100 spores. Plant material selected for ChIP-seq is boxed. (B) Relative

909 binding-peak distribution across genomic regions. The 1 kb region upstream of

910 the transcription start site (TSS) is defined as promoter. The fraction of

911 nucleotides in the complete At genome associated with each annotation type is



912 included in the figure as background control (At genome). (C) Distribution of

913 identified WRKY33 binding sites relative to the TSS. (D) Conserved DNA

914 elements enriched within the 500 bp WRKY33 binding peak regions identified

915 by DREME motif search. The TTGACT/C motif represents the well-established

916 W box, whereas T/GTTGAAT is an identified new motif.

917 **Figure 2.** WRKY33 regulated direct target genes in response to *B. cinerea*
918 2100 infection. (A) Number of differentially expressed genes (≥ 2 -fold; $P \leq 0.05$)
919 between WT and *wrky33* (*w33*) at 14 h after mock treatment (mo) or spray
920 inoculation with spores of *B. cinerea* 2100 (*B.c.*) identified by RNA-seq.
921 Indicated are total numbers (boxed) and numbers of up-regulated ()
922 and down-regulated genes () between treatments or genotypes. (B)
923 Venn diagram illustrating the total numbers and the number of common genes
924 affected in WT and *wrky33* 14 h post *B. cinerea* 2100 inoculation. (C) Venn
925 diagram showing the numbers of genes common to WRKY33-regulated genes
926 and WRKY33 target genes. (D) Percentage of WRKY33-repressed and
927 WRKY33-induced target genes (in total 318). (E) Enrichment of specific Gene
928 Ontology (GO) terms related to defense response, kinase activity, cell death,
929 and hormone responses among WRKY33-regulated target and non-target
930 genes (compared to the overall genome). The y-axis indicates the percentages
931 of genes associated to each GO category in each gene set. Asterisks indicate
932 significant enrichment (adj. p value < 0.05) of genes associated to the
933 respective GO term within a gene set as determined by GO term enrichment
934 analysis with goseq (null distribution approximated as Wallenius distribution;
935 correction for potential count biases via probability weighting).

936

937 **Figure 3.** WRKY33 regulated transcription factor families commonly

938 associated with stress responses. (A) WRKY, MYB, NAC and AP2/ERF TF
939 family genes are dominant targets of WRKY33 after *B. cinerea* 2100 infection.
940 The total number of members for each TF family is given in parenthesis next to
941 name. The number of WRKY33 directly or indirectly regulated family members
942 are indicated. (B, C) Integrative Genomics Viewer (IGV) images of ChIP-seq
943 data revealing high infection-dependent WRKY33 binding at the promoters of
944 *Arabidopsis* *WRKY33* (B) and *WRKY41* (C). Images for mock and *B.c.*
945 treatment of both biological repetitions are shown (1 and 2). Structure of the
946 targeted genes are indicated below along with the position of all W box motifs
947 within the loci. Arrows indicate direction of transcription. (D, E) qRT-PCR
948 analysis of *B. cinerea* 2100-induced expression of *WRKY33* (D) and *WRKY41*
949 (E) in WT and *wrky33* mutant plants at indicated time points post fungal spore
950 application. All data were normalized to the expression of At4g26410 and fold
951 induction values of all genes were calculated relative to the expression level of
952 mock treated (mo) WT plants set to 1. Error bars represent SD of three
953 biological replicates. Asterisks indicate significant differences between WT and
954 *wrky33* (*, $P < 0.05$; **, $P < 0.001$; two-tailed *t*-test). (F, G) Validation of ChIP-seq
955 data by ChIP-qPCR showing WRKY33 binding to its own promoter region (F)
956 and to the *WRKY41* promoter (G). WRKY33-HA (33HA) plants were spray
957 inoculated with spores of *B. cinerea* 2100 (Bc) or mock treated (mo) for 14 h.
958 Input DNA before immune precipitation (IN) and immune-precipitated DNA

959 using an anti-HA antibody (IP) were analyzed by qPCR employing
960 gene-specific primer pairs (p) indicated in the IGV graph. Shown is the fold
961 enrichment of bound DNA relative to a non-bound DNA fragment from
962 At2g04450. As a control for primer efficiency purified genomic DNA was
963 included in the analysis. Each ChIP experiment was repeated at least twice
964 with similar results.

965

966 **Figure 4.** WRKY33 directly regulates target genes encoding ABA biosynthetic
967 (*NCED3*, *NCED5*) and metabolic (*CYP707A3*) enzymes by binding to their
968 promoters or 3'UTR after *B. cinerea* 2100 treatment. (A, D, G) IGV
969 visualization of ChIP-seq data revealing infection-dependent WRKY33
970 enrichment at the *Arabidopsis NCED3* (A), *NCED5* (D) and *CYP707A3* (G) loci
971 with features described in Figure 3. (B, E, H) qRT-PCR analysis of *B. cinerea*
972 2100-induced expression of *NCED3* (B) *NCED5* (E) and *CYP707A3* (H) in WT
973 and *wrky33* as described in Figure 3. (C, F, I) Validation of the ChIP-seq data
974 for WRKY33 binding to the promoters of *NCED3* (C, with primer pairs p1 and
975 p2) and *CYP707A3* (I), and to the 3'UTR of *NCED5* (F) performed as
976 described the legend to Figure 3.

977

978 **Figure 5.** WRKY33 controls ABA-mediated plant susceptibility to *B. cinerea*
979 2100. (A) Growth phenotypes of WT, *wrky33*, *nced3 nced5*, and *wrky33 nced3*

980 *nced5 Arabidopsis* plants at 4 weeks under short day conditions. (B) *B. cinerea*
981 infection phenotypes 3 days post inoculation of WT, *wrky33*, *nced3*, *nced5*,
982 *nced3 nced5*, and *wrky33 nced3 nced5*. (C) *B. cinerea* biomass quantification
983 on indicated *Arabidopsis* genotypes. For fungal biomass determination the
984 relative abundance of *B. cinerea* and *Arabidopsis* DNA was determined by
985 qPCR employing specific primers for *BcCutinase A* and *AtSKII*, respectively.
986 (D) Exogenous application of ABA (10µM) directly to infection droplets on
987 *wrky33 nced3 nced5* leaves partially renders plants susceptible to *B. cinerea*
988 2100. Upon completion of the infection experiments (3 dpi), leaves were
989 detached and photographed. For all infections, two 2 µl droplets containing
990 2.5×10^5 spores were applied to each leaf.

991
992 **Figure 6.** Hormone levels in different genotypes during *B. cinerea* 2100
993 infection. Concentrations of the hormones ABA (A), SA (B), ACC (C) and JA
994 (D) were measured at 8, 14, 24 and 40 hpi in leaves of indicated *Arabidopsis*
995 genotypes spray inoculated with spores of *B. cinerea* 2100. Mock treated
996 plants (mo, 14 h) served as a control. The data show the average values and
997 SDs of the combined data from three independent experiments with up to four
998 replicates each.

999
1000 **Figure 7.** Expression of numerous genes up-regulated in infected *wrky33*

1001 plants showing WT-like levels in the *wrky33 nced3 nced5* triple mutant.
1002 Heatmap showing expression levels of genes, differentially expressed in
1003 RNA-seq and analyzed by qRT-PCR in WT, *wrky33 (w33)*, *nced3 nced5 (n3n5)*
1004 and *wrky33 nced3 nced5 (w33n3n5)* after mock treatment or 24 h post *B.*
1005 *cinerea* (*B.c.* 2100) infection. Genes showing high levels in *wrky33* but
1006 reduced levels in the triple mutant are boxed. All values were normalized to the
1007 expression of At4G26410.

1008

1009 **Figure 8.** Dual regulatory role of WRKY33 in modulating host defenses to *B.*
1010 *cinerea* 2100. WRKY33 positively regulates target genes involved in camalexin
1011 biosynthesis thereby contributing to host resistance towards *B. cinerea* 2100.
1012 Target genes involved in ET/JA biosynthesis and signaling can either be
1013 positively or negatively regulated by WRKY33. On the other hand, WRKY33
1014 negatively regulates ABA levels by i.e. directly targeting and repressing
1015 *NCED3* and *NCED5* expression, or inducing expression of *CYP707A3*, a gene
1016 involved in ABA metabolism. Thus, WRKY33 has both activator and repressor
1017 functions that may depend on promoter context. Red arrows indicate positive
1018 regulation whereas black bars indicate negative regulation. Curved red arrow
1019 highlights positive feedback regulation of WRKY33 on its own gene promoter.

1020

1021 **Figure 1 - figure supplement 1.** Conserved DNA elements within the 500 bp

1022 WRKY33 binding peak summit regions identified by MEME. (A) W-box with 5'
1023 extended motifs. (B) W-box with 3' extended motifs. (C) Additional conserved
1024 sequence GACTT/ATTC element. (D) Venn diagram illustrating the number of
1025 overlapping peaks containing both the W-box and the newly identified motif
1026 T/GTTGAAT.

1027

1028 **Figure 1 – figure supplement 2**

1029 WRKY33 does not bind to the G/TTTGAAT motif. EMSA was performed using
1030 recombinant WRKY33 and biotin labeled DNA probes. A DNA oligonucleotide
1031 containing 3 W-box elements (Mao *et al.*, 2011) or a W-box mutated version
1032 (W-boxmut) hereof served as a positive and as a negative control, respectively
1033 (A). The 45 bp M-3 was derived from the *PROPEP3* (At5g64905) gene
1034 promoter and contained three copies of the G/TTTGAAT motif, whereas the 40
1035 bp M-7 was derived from the *WAKL7* (At1g16090) gene promoter and
1036 contained one G/TTTGAAT motif. No binding of WRKY33 was observed to the
1037 W-boxmut probe and to both the M-3 and M-7 probes (B). Specificity of W-box
1038 binding was shown by competition assays using 250-fold (W-box) and 500-fold
1039 (W-box; M-3, M-7) excess of unlabeled probes. Protein lysates derived from
1040 IPTG-induced bacteria harboring the empty expression vector pMCSG48
1041 served as an additional control.

1042

1043 **Figure 2 - figure supplement 1.** GO graph visualization of top GO terms
1044 enriched among WRKY33-regulated WRKY33 target genes. (A) GO sub-graph
1045 induced by the top 10 GO terms in the category 'Biological Process'. (B) GO
1046 sub-graph induced by the top 5 GO terms in the category 'Molecular Function'.
1047 Boxes indicate the 10 (A) and 5 (B) most significant terms, respectively. Box
1048 color represents the relative significance, ranging from dark red (most
1049 significant) to light yellow (least significant). GO term enrichment was
1050 determined using goseq, with the null distribution approximated as Wallenius
1051 distribution and correcting for potential count biases via probability weighting.

1052

1053 **Figure 2 – figure supplement 2.** Analysis of WRKY33-regulated target genes
1054 from GO-terms hormone responses and cell death. (A) Venn diagram showing
1055 the overlap between the WRKY33-regulated target genes responsive to SA
1056 and associated with cell death. (B) The overlap of WRKY33-regulated target
1057 genes associated with the hormone pathways SA, ET, ABA and JA.

1058

1059 **Figure 3 - figure supplement 1.** Validation of WRKY33 directly regulated
1060 *WRKY* genes. Shown for each of the *WRKY* genes 38 (A), 48 (B), 50 (C),
1061 53(D), and 55 (E), are; i) the ChIP-seq data, visualized by the IGV browser,
1062 revealing strong infection-dependent WRKY33 enrichment at the
1063 corresponding promoter, ii) qRT-PCR analysis of *B. cinerea* 2100-induced

1064 expression of the respective *WRKY* gene in WT and *wrky33* at indicated time
1065 points post spore inoculation, and iii) ChIP-qPCR confirmation of WRKY33
1066 binding to the respective *WRKY* promoter. Amplicons used are indicated in the
1067 IGV images (p, p1, p2, p3). For detailed descriptions on how qRT-PCR and
1068 ChIP-qPCR were performed see legend to Figure 3.

1069

1070 **Figure 5 - figure supplement 1.** *B. cinerea* 2100 infection phenotypes of
1071 mature 4-week old leaves derived from *aba2-12* and *aba3-1* mutant plants.
1072 Pictures were taken 3 days post inoculation of two 2 µl droplets containing
1073 2.5×10^5 spores to each leaf (leaves were detached after completion of the
1074 experiment for photographic purposes only).

1075

1076 **Figure 5 - figure supplement 2.** *B. cinerea* 2100 infection phenotypes of
1077 mature 4-week old leaves derived from *wrky33 nced3* and *wrky33 nced5*
1078 mutant plants. Pictures were taken 3 days post inoculation of two 2 µl droplets
1079 containing 2.5×10^5 spores to each leaf (leaves were detached after completion
1080 of the experiment for photographic purposes only).

1081

1082 **Figure 5 – figure supplement 3.** Phenotype of WT Col-0 plants treated with
1083 ABA. Infection droplets with ABA (10µM; red arrows) or without ABA (black
1084 arrows) were applied to 4-week old leaves. No alteration of the WT resistant

1085 phenotype was observed. Picture was taken 3 days post inoculation of two 2 μ l
1086 droplets containing 2.5×10^5 spores to each leaf.

1087

1088 **Figure 5 - figure supplement 4.** *B. cinerea* 2100 infection phenotypes of
1089 mature 4-week old leaves derived from *cyp707a1*, *cyp707a2* and *cyp707a3*
1090 mutant plants. Pictures were taken 3 days post inoculation of two 2 μ l droplets
1091 containing 2.5×10^5 spores to each leaf (leaves were detached after completion
1092 of the experiment for photographic purposes only).

1093

1094 **Figure 8 - figure supplement 1.** Schematic representation showing of
1095 WRKY33-dependent host immunity towards the necrotroph *B. cinerea* 2100
1096 through repressing the ABA network. In WT *Arabidopsis* Col-0 plants (upper
1097 panel), *B. cinerea* inoculation induces *WRKY33* expression and protein
1098 accumulation that controls ABA levels by repressing the ABA biosynthetic
1099 target genes *NCED3* and *NCED5*, and by inducing the ABA metabolic gene
1100 *CYP707A3*. *WRKY33* also directly or indirectly represses expression of other
1101 genes in different hormone signaling pathways as well as genes encoding
1102 WRKY, and NAC TFs. *WRKY33* also positively affects resistance towards *B.*
1103 *cinerea* 2100 by directly targeting and inducing the expression of several genes
1104 involved in camalexin biosynthesis.
1105 In the *wrky33* mutant (lower panel) *B. cinerea* infection fails to activate host

1106 camalexin biosynthesis genes and increases ABA levels by up-regulation of
1107 *NCED3* and *NCED5*, which activates downstream ABA-dependent genes and
1108 ABA signaling. Among the ABA-dependent genes are genes involved in SA
1109 signaling, WRKY TFs, NAC TFs, and genes associated with auxin or JA
1110 conjugation indicating that ABA may acts as a key sub-node in
1111 WRKY33-dependent host immunity to *B. cinerea*.
1112 Whereas WT-like resistance is restored in the *wrky33 nced3 nced5* triple
1113 mutant, all currently tested mutants of WRKY33 regulated genes acting
1114 downstream of ABA failed to restore resistance in the *wrky33* mutant
1115 background (marked by an asterisk). Thus, additional crucial genes causal for
1116 WRKY33-dependent resistance to *B. cinerea* 2100 remain to be discovered, as
1117 do ABA signaling components affecting *WRKY33* expression (indicated by the
1118 question marks). The solid lines with arrows indicate induction or positive
1119 modulation, the bar heads indicate suppression. Direct WRKY33 targets are
1120 indicated by the green color.

1121

1122 **Figure 8 – figure supplement 2.** *AMT1* and *CYP71A12* expression is
1123 positively regulated by WRKY33. (A-B) Integrative Genomics Viewer (IGV)
1124 images of ChIP-seq data revealing high infection-dependent WRKY33 binding
1125 at the promoters of *AMT1* (A) and *CYP71A12* (B). (C-D) qRT-PCR analyses of
1126 *AMT1* (C) and *CYP71A12* (D) in WT and *wrky33* at the indicated time points

1127 after *B. cinerea* 2100 spore inoculation. qRT-PCR data were normalized to the
1128 expression of At4g26410. Error bars represent SD of three biological replicates
1129 (n=3). Asterisks indicate significant differences between WT and *wrky33* (*,
1130 $P < 0.05$; **, $P < 0.001$; two-tailed *t*-test).

1131

1132 **Figure 8 – figure supplement 3.** The role of *GH3* genes in
1133 WRKY33-mediated host resistance to *B. cinerea* 2100. (A) Expression levels
1134 of *GH3.2* and *GH3.3* in WT and *wrky33* plants determined by qRT-PCR at the
1135 indicated time points after *B. cinerea* 2100 spore inoculation. Data were
1136 normalized to the expression of At4g26410. Error bars represent SD of three
1137 biological replicates (n=3). Asterisks indicate significant differences between
1138 WT and *wrky33* (*, $P < 0.05$; **, $P < 0.001$; two-tailed *t*-test). (B) *B. cinerea* 2100
1139 infection phenotypes of WT, *wrky33*, *gh3.2*, *gh3.3*, *gh3.2 gh3.3* and *wrky33*
1140 *gh3.2 gh3.3* plants are shown at 3 days post infection. Two 2 μ l droplets
1141 containing 2.5×10^5 spores were applied to each leaf.

1142

1143 **Supplementary file 1.** Summary of identified WRKY33 binding sites 14 h post
1144 *B. cinerea* 2100 inoculation.

1145 **Supplementary file 2.** List of confirmed WRKY33 target genes.

1146 **Supplementary file 3.** List of WRKY33 regulated target genes involved in cell
1147 death.

1148 **Supplementary file 4.** List of WRKY33 regulated target genes associated in
1149 the GO category “kinase activity”.

1150 **Supplementary file 5.** List of WRKY33 target genes encoding transcription
1151 factors.

1152 **Supplementary file 6.** List of primers used for genotyping.

1153 **Supplementary file 7.** List of primers used for ChIP-qPCR.

1154 **Supplementary file 8.** List of primers used for qRT-PCR.

1155

1156 **Source code 1.** R function to identify overlapping peak regions.

1157

1158 **References**

1159 Adie BAT, Perez-Perez J, Perez-Perez MM, Godoy M, Sanchez-Serrano J-J,
1160 Schmelz EA , Solano R. 2007. ABA is an essential signal for plant
1161 resistance to pathogens affecting JA biosynthesis and the activation of
1162 defenses in Arabidopsis. *The Plant Cell* **19**:1665-1681.

1163 Alexandre C , Vincent J-P. 2003. Requirements for transcriptional repression
1164 and activation by Engrailed in *Drosophila* embryos. *Development*
1165 **130**:729-739. 10.1242/dev.00286

1166 Andreasson E, Jenkins T, Brodersen P, Thorgrimsen S, Petersen NHT, Zhu S,
1167 Qiu, J.-L., Micheelsen P, Rocher A, Petersen M, Newman M-A, Nielsen
1168 HB, Hirt H, Somssich I, Mattsson O , Mundy J. 2005. The MAP kinase

1169 substrate MKS1 is a regulator of plant defense responses. *The EMBO*
1170 *Journal* **24**:2579-2589.

1171 Asselbergh B, De Vleeschauwer D , Höfte M. 2008. Global switches and
1172 fine-tuning - ABA modulates plant pathogen defense. *Molecular*
1173 *Plant-Microbe Interactions* **21**:709-719.

1174 Bari R , Jones J. 2009. Role of plant hormones in plant defence responses.
1175 *Plant Molecular Biology* **69**:473-488.

1176 Berger N , Dubreucq B. 2012. Evolution goes GAGA: GAGA binding proteins
1177 across kingdoms. *Biochimica et Biophysica Acta (BBA) - Gene*
1178 *Structure and Expression* **1819**:863-868.
1179 <http://dx.doi.org/10.1016/j.bbagr.2012.02.022>

1180 Berrocal-Lobo M, Molina A , Solano R. 2002. Constitutive expression of
1181 *ETHYLENE-RESPONSE-FACTOR1* in *Arabidopsis* confers resistance
1182 to several necrotrophic fungi. *The Plant Journal* **29**:23-32.

1183 Birkenbihl RP, Diezel C , Somssich IE. 2012. Arabidopsis WRKY33 is a key
1184 transcriptional regulator of hormone and metabolic responses towards
1185 *Botrytis cinerea* infection. . *Plant Physiology* **159**:266-285.

1186 Birkenbihl RP , Somssich IE. 2011. Transcriptional plant responses critical for
1187 resistance towards necrotrophic pathogens. *Frontiers in Plant Science*
1188 **2**:76.

1189 Bu Q, Jiang H, Li C-B, Zhai Q, Zhang J, Wu X, Sun J, Xie Q , Li C. 2008. Role

1190 of the *Arabidopsis thaliana* NAC transcription factors ANAC019 and
1191 ANAC055 in regulating jasmonic acid-signaled defense responses. *Cell*
1192 *Research* **18**:756-767.

1193 Chang K, Zhong S, Weirauch M, Hon G, Pelizzola M, Li H, Huang S-s, Schmitz
1194 R, Urich MA, Kuo D, Nery J, Qiao H, Yang A, Jamali A, Chen H, Ideker
1195 T, Ren B, Bar-Joseph Z, Hughes T , Ecker J. 2013. Temporal
1196 transcriptional response to ethylene gas drives growth hormone
1197 cross-regulation in *Arabidopsis*. *eLife* **2** 00675. DOI:
1198 10.7554/eLife.00675

1199 Cheng Y, Zhou Y, Yang Y, Chi Y-J, Zhou J, Chen J-Y, Wang F, Fan B, Shi K,
1200 Zhou Y-H, Yu J-Q , Chen Z. 2012. Structural and functional analysis of
1201 VQ motif-containing proteins in *Arabidopsis* as interacting proteins of
1202 WRKY transcription factors. *Plant Physiology* **159**:810-825.

1203 Ciolkowski I, Wanke D, Birkenbihl R , Somssich IE. 2008. Studies on
1204 DNA-binding selectivity of WRKY transcription factors lend structural
1205 clues into WRKY-domain function. *Plant Molecular Biology* **68**:81-92.

1206 Cusanovich DA, Pavlovic B, Pritchard JK , Gilad Y. 2014. The functional
1207 consequences of variation in transcription factor binding. *PLoS*
1208 *Genetics* **10**:e1004226. 10.1371/journal.pgen.1004226

1209 Czechowski T, Stitt M, Altmann T, Udvardi MK , Scheible W-R. 2005.
1210 Genome-wide identification and testing of superior reference genes for

1211 transcript normalization in *Arabidopsis*. *Plant Physiology* **139**:5-17.

1212 de Torres-Zabala M, Truman W, Bennett MH, Lafforgue G, Mansfield JW,
1213 Rodriguez Egea P, Bögre L , Grant M. 2007. *Pseudomonas syringae* pv.
1214 *tomato* hijacks the *Arabidopsis* abscisic acid signalling pathway to
1215 cause disease. *The EMBO Journal* **26**:1434-1443.

1216 Dean R, Van Kan JAL, Pretorius ZA, Hammond-Kosack KE, Di Pietro A, Spanu
1217 PD, Rudd JJ, Dickman M, Kahmann R, Ellis J , Foster GD. 2012. The
1218 Top 10 fungal pathogens in molecular plant pathology. *Molecular Plant*
1219 *Pathology* **13**:414-430. 10.1111/j.1364-3703.2011.00783.x

1220 Eulgem T. 2006. Dissecting the WRKY web of plant defense regulators. *PLoS*
1221 *Pathogens* **2**:e126.

1222 Fan M, Bai M-Y, Kim J-G, Wang T, Oh E, Chen L, Park CH, Son S-H, Kim S-K,
1223 Mudgett MB , Wang Z-Y. 2014. The bHLH transcription factor HBI1
1224 mediates the trade-off between growth and pathogen-associated
1225 molecular pattern–triggered immunity in *Arabidopsis*. *The Plant Cell*
1226 **26**:828-841. 10.1105/tpc.113.121111

1227 Finkelstein R. 2013. Abscisic acid synthesis and response. *The Arabidopsis*
1228 *Book* **11**:e0166. 10.1199/tab.0166

1229 Frey A, Effroy D, Lefebvre V, Seo M, Perreau F, Berger A, Sechet J, To A,
1230 North HM , Marion-Poll A. 2012. Epoxycarotenoid cleavage by NCED5
1231 fine-tunes ABA accumulation and affects seed dormancy and drought

1232 tolerance with other NCED family members. *The Plant Journal*
1233 **70**:501-512. 10.1111/j.1365-313X.2011.04887.x

1234 Gachon C , Saindrenan P. 2004. Real-time PCR monitoring of fungal
1235 development in *Arabidopsis thaliana* infected by *Alternaria brassicicola*
1236 and *Botrytis cinerea*. *Plant Physiology and Biochemistry* **42**:367-371.

1237 Gendrel A-V, Lippman Z, Martienssen R , Colot V. 2005. Profiling histone
1238 modification patterns in plants using genomic tiling microarrays. *Nature*
1239 *Methods* **2**:213-218.

1240 Glazebrook J. 2005. Contrasting mechanisms of defense against biotrophic
1241 and necrotrophic pathogens. *Annual Reviews of Phytopathology*
1242 **43**:205-227.

1243 Gonzalez-Lamothe R, Boyle P, Dulude A, Roy V, Lezin-Doumbou C, Kaur GS,
1244 Bouarab K, Despres C , Brisson N. 2008. The transcriptional activator
1245 Pti4 is required for the recruitment of a repressosome nucleated by
1246 repressor SEBF at the potato *PR-10a* gene. *The Plant Cell*
1247 **20**:3136-3147.

1248 González-Lamothe R, El Oirdi M, Brisson N , Bouarab K. 2012. The
1249 conjugated auxin indole-3-acetic acid - aspartic acid promotes plant
1250 disease development. *The Plant Cell* **24**:762-777.

1251 Grant C, Bailey T , Noble W. 2011. FIMO: scanning for occurrences of a given
1252 motif. *Bioinformatics* **27**:1017 - 1018.

1253 Gutierrez L, Mongelard G, Floková K, Păcurar DI, Novák O, Staswick P,
1254 Kowalczyk M, Păcurar M, Demailly H, Geiss G , Bellini C. 2012. Auxin
1255 controls *Arabidopsis* adventitious root initiation by regulating jasmonic
1256 acid homeostasis. *The Plant Cell Online* **24**:2515-2527.
1257 10.1105/tpc.112.099119

1258 Han L, Li GJ, Yang KY, Mao G, Wang R, Liu Y , Zhang S. 2010.
1259 Mitogen-activated protein kinase 3 and 6 regulate *Botrytis*
1260 *cinerea*-induced ethylene production in *Arabidopsis*. *The Plant Journal*
1261 **64**:114-127.

1262 Heinz S, Benner C, Spann N, Bertolino E, Lin YC, Laslo P, Cheng JX, Murre C,
1263 Singh H , Glass CK. 2010. Simple combinations of lineage-determining
1264 transcription factors prime *cis*-regulatory elements required for
1265 macrophage and B cell identities. *Molecular Cell* **38**:576-589.
1266 <http://dx.doi.org/10.1016/j.molcel.2010.05.004>

1267 Hu P, Zhou W, Cheng Z, Fan M, Wang L , Xie D. 2013. JAV1 controls
1268 jasmonate-regulated plant defense. *Molecular Cell* **50**:504-515.

1269 Huang P-Y, Yeh Y-H, Liu A-C, Cheng C-P , Zimmerli L. 2014. The *Arabidopsis*
1270 LecRK-VI.2 associates with the pattern-recognition receptor FLS2 and
1271 primes *Nicotiana benthamiana* pattern-triggered immunity. *The Plant*
1272 *Journal* **79**:243-255. 10.1111/tpj.12557

1273 Ikeda M, Mitsuda N , Ohme-Takagi M. 2009. Arabidopsis WUSCHEL is a

1274 bifunctional transcription factor that acts as a repressor in stem cell
1275 regulation and as an activator in floral patterning. *The Plant Cell*
1276 **21**:3493-3505. 10.1105/tpc.109.069997

1277 Jensen MK, Hagedorn PH, De Torres-Zabala M, Grant MR, Rung JH, Collinge
1278 DB , Lyngkjaer MF. 2008. Transcriptional regulation by an NAC
1279 (NAM-ATAF1,2-CUC2) transcription factor attenuates ABA signalling
1280 for efficient basal defence towards *Blumeria graminis* f. sp. *hordei* in
1281 *Arabidopsis*. *The Plant Journal* **56**:867-880.
1282 10.1111/j.1365-313X.2008.03646.x

1283 Jensen MK, Lindemose S, Masi Fd, Reimer JJ, Nielsen M, Perera V, Workman
1284 CT, Turck F, Grant MR, Mundy J, Petersen M , Skriver K. 2013. ATAF1
1285 transcription factor directly regulates abscisic acid biosynthetic gene
1286 *NCED3* in *Arabidopsis thaliana*. *FEBS Open Bio* **3**:321-327.
1287 <http://dx.doi.org/10.1016/j.fob.2013.07.006>

1288 Jiang H, Li H, Bu Q , Li C. 2009. The RHA2a-interacting proteins ANAC019
1289 and ANAC055 may play a dual role in regulating ABA response and
1290 jasmonate response. *Plant Signaling & Behavior* **4**:464-466.

1291 Kazan K , Manners JM. 2013. MYC2: The master in action. *Molecular Plant*
1292 **6**:686-703

1293 Kim D, Pertea G, Trapnell C, Pimentel H, Kelley R , Salzberg S. 2013.
1294 TopHat2: accurate alignment of transcriptomes in the presence of

1295 insertions, deletions and gene fusions. *Genome Biology* **14**:R36.

1296 Kliebenstein DJ, Rowe HC , Denby KJ. 2005. Secondary metabolites influence

1297 Arabidopsis/Botrytis interactions: variation in host production and

1298 pathogen sensitivity. *The Plant Journal* **44**:25-36.

1299 Lai Z, Li Y, Wang F, Cheng Y, Fan B, Yu J-Q , Chen Z. 2011. Arabidopsis sigma

1300 factor binding proteins are activators of the WRKY33 transcription factor

1301 in plant defense. *The Plant Cell* **23**:3824-3841.

1302 Langmead B, Trapnell C, Pop M , Salzberg S. 2009. Ultrafast and

1303 memory-efficient alignment of short DNA sequences to the human

1304 genome. *Genome Biology* **10**:R25.

1305 Law C, Chen Y, Shi W , Smyth G. 2014. voom: precision weights unlock linear

1306 model analysis tools for RNA-seq read counts. *Genome Biology*

1307 **15**:R29.

1308 Łażniewska J, Macioszek V, Lawrence C , Kononowicz A. 2010. Fight to the

1309 death: *Arabidopsis thaliana* defense response to fungal necrotrophic

1310 pathogens. *Acta Physiologiae Plantarum* **32**:1-10.

1311 Leng P, Yuan B, Guo Y , Chen P. 2014. The role of abscisic acid in fruit

1312 ripening and responses to abiotic stress. *Journal of Experimental*

1313 *Botany*:in press. 10.1093/jxb/eru204

1314 Léon-Kloosterziel KM, Gil MA, Ruijs GJ, Jacobsen SE, Olszewski NE,

1315 Schwartz SH, Zeevaart JAD , Koornneef M. 1996. Isolation and

1316 characterization of abscisic acid-deficient Arabidopsis mutants at two
1317 new loci. *The Plant Journal* **10**:655-661.
1318 10.1046/j.1365-313X.1996.10040655.x

1319 Li G, Meng X, Wang R, Mao G, Han L, Liu Y , Zhang S. 2012. Dual-level
1320 regulation of ACC synthase activity by MPK3/MPK6 cascade and its
1321 downstream WRKY transcription factor during ethylene induction in
1322 *Arabidopsis*. *PLoS Genetics* **8**:e1002767.

1323 Lippok B, Birkenbihl RP, Rivory G, Brümmer J, Schmelzer E, Logemann E ,
1324 Somssich IE. 2007. Expression of *AtWRKY33* encoding a
1325 pathogen-/PAMP-responsive WRKY transcription factor is regulated by
1326 a composite DNA motif containing W box elements. . *Molecular*
1327 *Plant-Microbe Interactions* **20**:420-429.

1328 Llorca CM, Potschin M , Zentgraf U. 2014. bZIPS and WRKYs: two large
1329 transcription factor families executing two different functional strategies.
1330 *Frontiers in Plant Science* **5**:169. 10.3389/fpls.2014.00169

1331 Luo H, Laluk K, Lai Z, Veronese P, Song F , Mengiste T. 2010. The Arabidopsis
1332 Botrytis Susceptible1 Interactor defines a subclass of RING E3 ligases
1333 that regulate pathogen and stress responses. *Plant Physiology*
1334 **154**:1766-1782.

1335 Machanick P , Bailey T. 2011. MEME-ChIP: motif analysis of large DNA
1336 datasets. *Bioinformatics* **27**:1696 - 1697.

1337 Machens F, Becker M, Umrath F , Hehl R. 2014. Identification of a novel type
1338 of WRKY transcription factor binding site in elicitor-responsive
1339 *cis*-sequences from *Arabidopsis thaliana*. *Plant Molecular Biology*
1340 **84**:371-385. 10.1007/s11103-013-0136-y

1341 MacQuarrie KL, Fong AP, Morse RH , Tapscott SJ. 2011. Genome-wide
1342 transcription factor binding: beyond direct target regulation. *Trends in*
1343 *Genetics* **27**:141-148. <http://dx.doi.org/10.1016/j.tig.2011.01.001>

1344 Mao G, Meng X, Liu Y, Zheng Z, Chen Z , Zhang S. 2011. Phosphorylation of a
1345 WRKY Transcription Factor by Two Pathogen-Responsive MAPKs
1346 Drives Phytoalexin Biosynthesis in *Arabidopsis*. *The Plant Cell*
1347 **23**:1639-1653.

1348 Martin M. 2011. Cutadapt removes adapter sequences from high-throughput
1349 sequencing reads. *EMBnet.journal* **17**:10-12. 10.14806/ej.17.1.200
1350 pp. 10-12

1351 Mengiste T. 2012. Plant immunity to necrotrophs. *Annual Review of*
1352 *Phytopathology* **50**:267-294.
1353 doi:10.1146/annurev-phyto-081211-172955

1354 Miao Y, Laun T, Zimmermann P , Zentgraf U. 2004. Targets of the WRKY53
1355 transcription factor and its role during leaf senescence in *Arabidopsis*.
1356 *Plant Molecular Biology* **55**:853-867.

1357 Miyakawa T, Fujita Y, Yamaguchi-Shinozaki K , Tanokura M. 2013. Structure

1358 and function of abscisic acid receptors. *Trends in Plant Science*
1359 **18**:259-266.

1360 Moffat CS, Ingle RA, Wathugala DL, Saunders NJ, Knight H , Knight MR. 2012.
1361 ERF5 and ERF6 play redundant roles as positive regulators of
1362 JA/Et-mediated defense against *Botrytis cinerea* in Arabidopsis. *PLoS*
1363 *ONE* **7**:e35995.

1364 Nafisi M, Goregaoker S, Botanga CJ, Glawischnig E, Olsen CE, Halkier BA ,
1365 Glazebrook J. 2007. Arabidopsis cytochrome P450 monooxygenase
1366 71A13 catalyzes the conversion of indole-3-acetaldoxime in camalexin
1367 synthesis. *The Plant Cell* **19**:2039-2052.

1368 Nurmberg PL, Knox KA, Yun B-W, Morris PC, Shafiei R, Hudson A , Loake GJ.
1369 2007. The developmental selector *AS1* is an evolutionarily conserved
1370 regulator of the plant immune response. *Proceedings of the National*
1371 *Academy of Sciences of the United States of America*
1372 **104**:18795-18800.

1373 Pandey SP , Somssich IE. 2009. The role of WRKY transcription factors in
1374 plant immunity. *Plant Physiology* **150**:1648-1655.

1375 Pecher P, Eschen-Lippold L, Herklotz S, Kuhle K, Naumann K, Bethke G, Uhrig
1376 J, Weyhe M, Scheel D , Lee J. 2014. The *Arabidopsis thaliana*
1377 mitogen-activated protein kinases MPK3 and MPK6 target a subclass of
1378 'VQ-motif'-containing proteins to regulate immune responses. *New*

- 1379 *Phytologist* **203**:592-606. 10.1111/nph.12817
- 1380 Pieterse CMJ, Leon-Reyes A, Van der Ent S , Van Wees SCM. 2009.
- 1381 Networking by small-molecule hormones in plant immunity. *Nature*
- 1382 *Chemical Biology* **5**:308-316.
- 1383 Pré M, Atallah M, Champion A, De Vos M, Pieterse CMJ , Memelink J. 2008.
- 1384 The AP2/ERF domain transcription factor ORA59 integrates jasmonic
- 1385 acid and ethylene signals in plant defense. *Plant Physiology*
- 1386 **147**:1347-1357.
- 1387 Qiu J-L, Fill B-K, Petersen K, Nielsen HB, Botanga CJ, Thorgrimsen S, Palma
- 1388 K, Suarez-Rodriguez MC, Sandbech-Clausen S, Lichota J, Brodersen
- 1389 P, Grasser KD, Mattsson O, Glazebrook J, Mundy J , Petersen M. 2008.
- 1390 *Arabidopsis* MAP kinase 4 regulates gene expression through
- 1391 transcription factor release in the nucleus. *The EMBO Journal*
- 1392 **27**:2214-2221.
- 1393 Quinlan A , Hall I. 2010. BEDTools: a flexible suite of utilities for comparing
- 1394 genomic features. *Bioinformatics* **26**:841 - 842.
- 1395 Ramírez V, Agorio A, Coego A, García-Andrade J, Hernández MJ, Balaguer B,
- 1396 Ouwerkerk PBF, Zarra I , Vera P. 2011. MYB46 modulates disease
- 1397 susceptibility to *Botrytis cinerea* in *Arabidopsis*. *Plant Physiology*
- 1398 **155**:1920-1935.
- 1399 Robatzek S , Somssich IE. 2002. Targets of AtWRKY6 regulation during plant

1400 senescence and pathogen defense. *Genes & Development*
1401 **16**:1139-1149.

1402 Robert-Seilaniantz A, Grant M , Jones JDG. 2011. Hormone crosstalk in plant
1403 disease and defense: More than just JASMONATE-SALICYLATE
1404 antagonism. *Annual Review of Phytopathology* **49**:317-343.

1405 Robinson MD, McCarthy DJ , Smyth GK. 2010. edgeR: a Bioconductor
1406 package for differential expression analysis of digital gene expression
1407 data. *Bioinformatics* **26**:139-140. 10.1093/bioinformatics/btp616

1408 Rowe HC , Kliebenstein DJ. 2008. Complex genetics control natural variation
1409 in *Arabidopsis thaliana* resistance to *Botrytis cinerea*. *Genetics*
1410 **180**:2237-2250.

1411 Rushton PJ, Somssich IE, Ringler P , Shen QJ. 2010. WRKY transcription
1412 factors. *Trends in Plant Science* **15**:247-258.

1413 Sakabe NJ, Aneas I, Shen T, Shokri L, Park S-Y, Bulyk ML, Evans SM ,
1414 Nobrega MA. 2012. Dual transcriptional activator and repressor roles of
1415 TBX20 regulate adult cardiac structure and function. *Human Molecular*
1416 *Genetics* **21**:2194-2204. 10.1093/hmg/dds034

1417 Sánchez-Vallet A, López G, Ramos B, Delgado-Cerezo M, Riviere M-P,
1418 Llorente F, Fernández PV, Miedes E, Estevez JM, Grant M , Molina A.
1419 2012. Disruption of abscisic acid signaling constitutively activates
1420 *Arabidopsis* resistance to the necrotrophic fungus *Plectosphaerella*

1421 *cucumerina*. *Plant Physiology* **160**:2109-2124. 10.1104/pp.112.200154

1422 Sánchez-Vallet A, Ramos B, Bednarek P, López G, Piślewska-Bednarek M,
1423 Schulze-Lefert P , Molina A. 2010. Tryptophan-derived secondary
1424 metabolites in *Arabidopsis thaliana* confer non-host resistance to
1425 necrotrophic *Plectosphaerella cucumerina* fungi. *The Plant Journal*
1426 **63**:115-127. 10.1111/j.1365-313X.2010.04224.x

1427 Schmieder R , Edwards R. 2011. Quality control and preprocessing of
1428 metagenomic datasets. *Bioinformatics* **27**:863-864.
1429 10.1093/bioinformatics/btr026

1430 Shankaranarayanan P, Mendoza-Parra M-A, Walia M, Wang L, Li N, Trindade
1431 LM , Gronemeyer H. 2011. Single-tube linear DNA amplification (LinDA)
1432 for robust ChIP-seq. *Nature Methods* **8**:565-567.

1433 Singh P, Kuo Y-C, Mishra S, Tsai C-H, Chien C-C, Chen C-W,
1434 Desclos-Theveniau M, Chu P-W, Schulze B, Chinchilla D, Boller T ,
1435 Zimmerli L. 2012. The lectin receptor kinase-VI.2 is required for priming
1436 and positively regulates *Arabidopsis* pattern-triggered immunity. *The*
1437 *Plant Cell* **24**:1256-1270.

1438 Ton J, Flors V , Mauch-Mani B. 2009. The multifaceted role of ABA in disease
1439 resistance. *Trends in Plant Science* **14**:310-317.
1440 <http://dx.doi.org/10.1016/j.tplants.2009.03.006>

1441 Valouev A, Johnson DS, Sundquist A, Medina C, Anton E, Batzoglou S, Myers

1442 RM , Sidow A. 2008. Genome-wide analysis of transcription factor
1443 binding sites based on ChIP-Seq data. *Nature Methods* **5**:829-834.

1444 Wang Xe, Basnayake BMVS, Zhang H, Li G, Li W, Virk N, Mengiste T , Song F.
1445 2009. The Arabidopsis ATAF1, a NAC transcription factor, is a negative
1446 regulator of defense responses against necrotrophic fungal and
1447 bacterial pathogens. *Molecular Plant-Microbe Interactions*
1448 **22**:1227-1238.

1449 Williamson B, Tudzynski B, Tudzynski P , Van Kan JAL. 2007. *Botrytis cinerea*:
1450 the cause of grey mould disease. *Molecular Plant Pathology* **8**:561-580.

1451 Windram O, Madhou P, McHattie S, Hill C, Hickman R, Cooke E, Jenkins DJ,
1452 Penfold CA, Baxter L, Breeze E, Kiddle SJ, Rhodes J, Atwell S,
1453 Kliebenstein DJ, Kim Y-s, Stegle O, Borgwardt K, Zhang C, Tabrett A,
1454 Legaie R, Moore J, Finkenstadt B, Wild DL, Mead A, Rand D, Beynon J,
1455 Ott S, Buchanan-Wollaston V , Denby KJ. 2012. Arabidopsis defense
1456 against *Botrytis cinerea*: chronology and regulation deciphered by
1457 high-resolution temporal transcriptomic analysis. *The Plant Cell*
1458 **24**:3530-3557.

1459 Yamaguchi Y, Huffaker A, Bryan AC, Tax FE , Ryan CA. 2010. PEPR2 is a
1460 second receptor for the Pep1 and Pep2 peptides and contributes to
1461 defense responses in *Arabidopsis*. *The Plant Cell* **22**:508-522.

1462 Young M, Wakefield M, Smyth G , Oshlack A. 2010. Gene ontology analysis for

1463 RNA-seq: accounting for selection bias. *Genome Biology* **11**:R14.

1464 Yu X, Li L, Zola J, Aluru M, Ye H, Foudree A, Guo H, Anderson S, Aluru S, Liu
1465 P, Rodermel S , Yin Y. 2011. A brassinosteroid transcriptional network
1466 revealed by genome-wide identification of BES1 target genes in
1467 *Arabidopsis thaliana*. *The Plant Journal* **65**:634-646.

1468 Zander M, Thurow C , Gatz C. 2014. TGA transcription factors activate the
1469 salicylic acid-suppressible branch of the ethylene-induced defense
1470 program by regulating *ORA59* expression. *Plant Physiology*
1471 **165**:1671-1683. 10.1104/pp.114.243360

1472 Zhao Y, Wei T, Yin K-Q, Chen Z, Gu H, Qu L-J , Qin G. 2012. Arabidopsis
1473 RAP2.2 plays an important role in plant resistance to *Botrytis cinerea*
1474 and ethylene responses. *New Phytologist* **195**:450-460.
1475 10.1111/j.1469-8137.2012.04160.x

1476 Zheng X-y, Spivey Natalie W, Zeng W, Liu P-P, Fu Zheng Q, Klessig Daniel F,
1477 He Sheng Y , Dong X. 2012. Coronatine promotes *Pseudomonas*
1478 *syringae* virulence in plants by activating a signaling cascade that
1479 inhibits salicylic acid accumulation. *Cell Host & Microbe* **11**:587-596.
1480 10.1016/j.chom.2012.04.014

1481 Zheng Z, Qamar SA, Chen Z , Mengiste T. 2006. Arabidopsis WRKY33
1482 transcription factor is required for resistance to necrotrophic fungal
1483 pathogens. *The Plant Journal* **48**:592-605.

1484 Zhou N, Tootle TL , Glazebrook J. 1999. Arabidopsis *PAD3*, a gene required for
1485 camalexin biosynthesis, encodes a putative cytochrome P450
1486 monooxygenase. *The Plant Cell* **11**:2419-2428.

1487 Zhu X, Wang Y, Pi W, Liu H, Wickrema A , Tuan D. 2012. NF-Y recruits both
1488 transcription activator and repressor to modulate tissue- and
1489 developmental stage-specific expression of human γ -globin gene. *PLoS*
1490 *ONE* **7**:e47175. 10.1371/journal.pone.0047175

1491 Ziegler J, Qwegwer J, Schubert M, Erickson JL, Schattat M, Bürstenbinder K,
1492 Grubb CD , Abel S. 2014. Simultaneous analysis of apolar
1493 phytohormones and 1-aminocyclopropan-1-carboxylic acid by high
1494 performance liquid chromatography/electrospray negative ion tandem
1495 mass spectrometry via 9-fluorenylmethoxycarbonyl chloride
1496 derivatization. *Journal of Chromatography A* **1362**:102-109.
1497 <http://dx.doi.org/10.1016/j.chroma.2014.08.029>
1498
1499

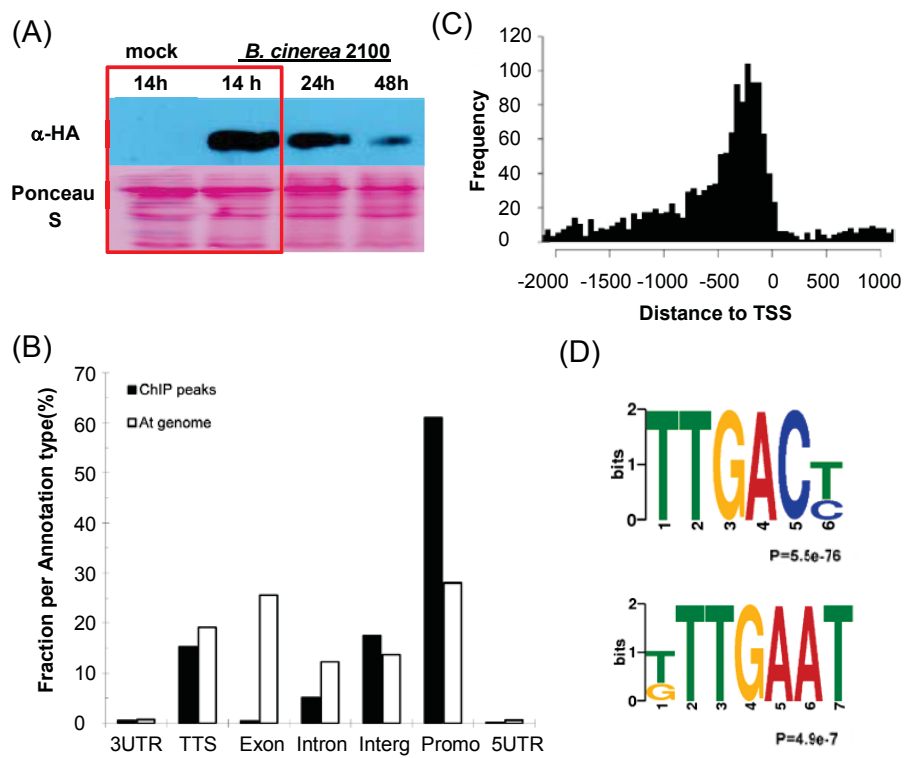


Figure 1

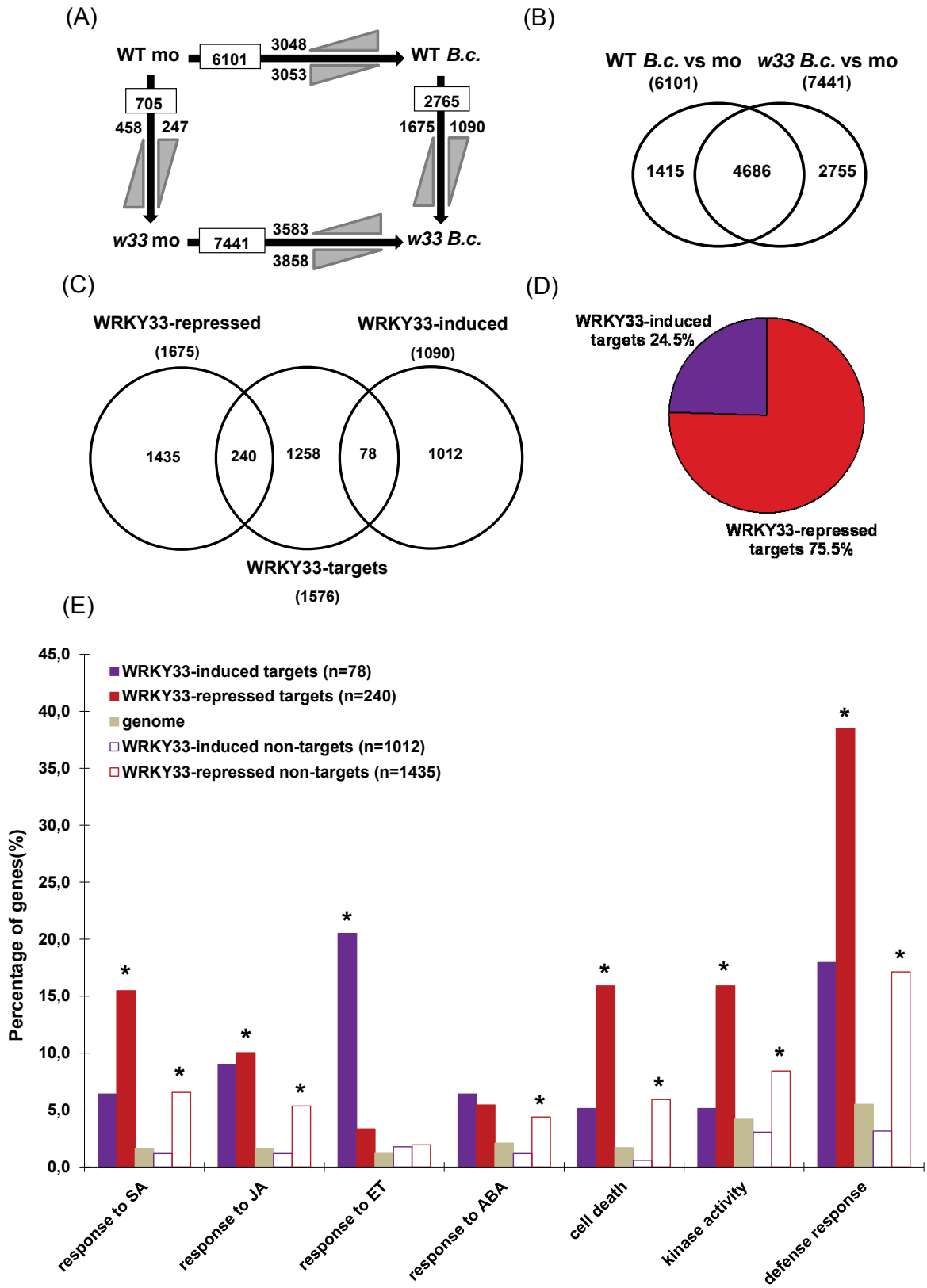


Figure 2

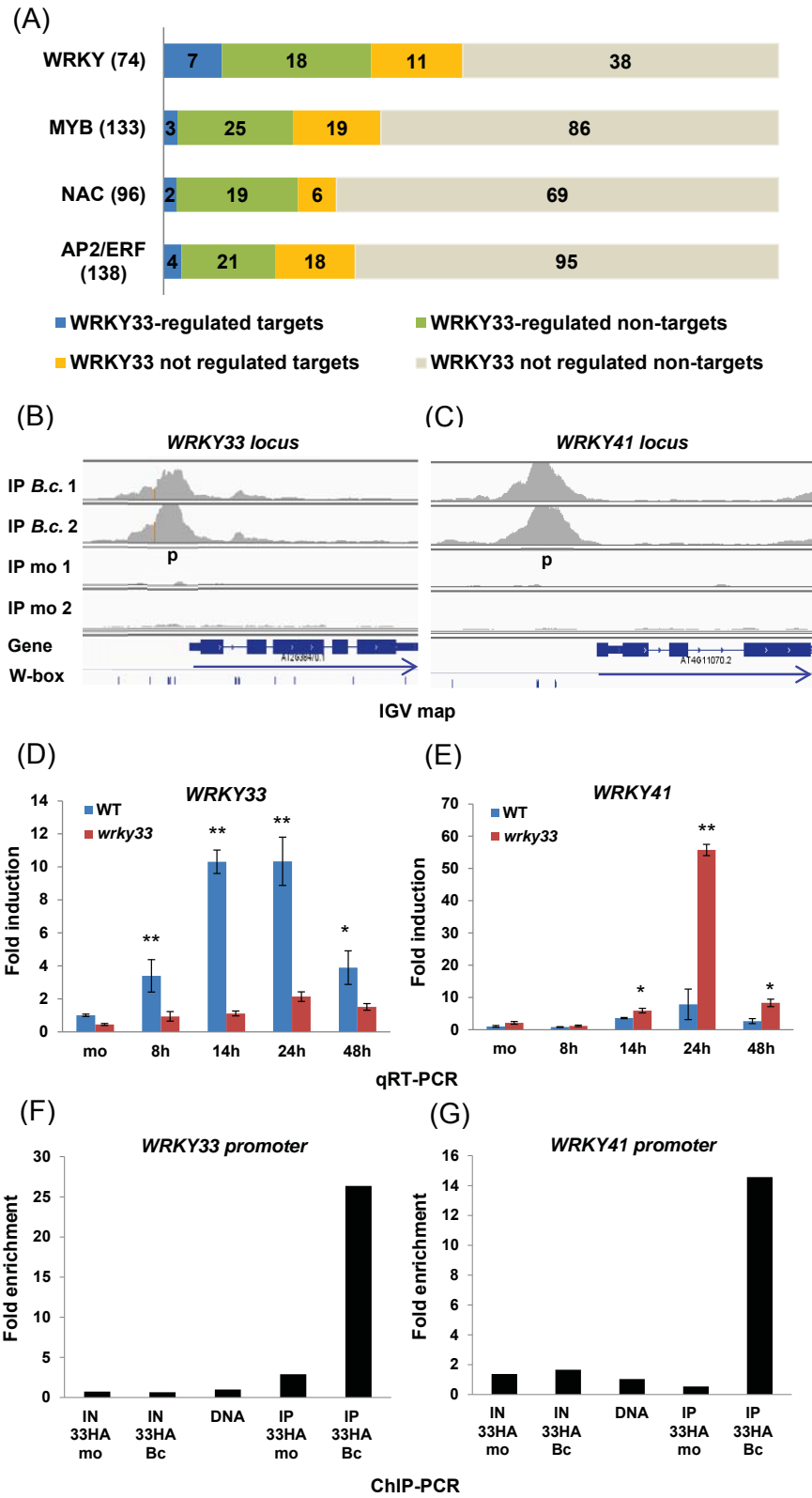


Figure 3

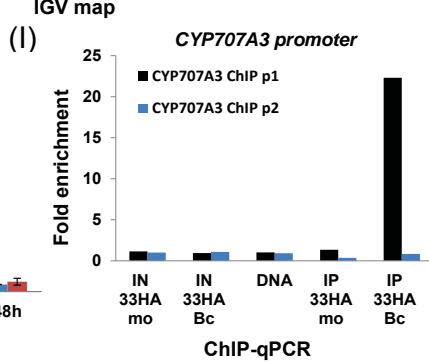
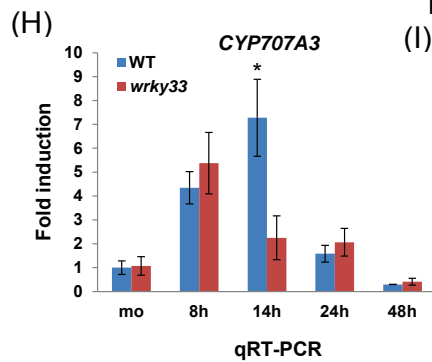
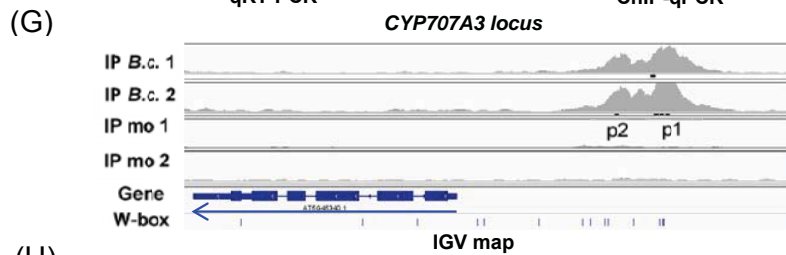
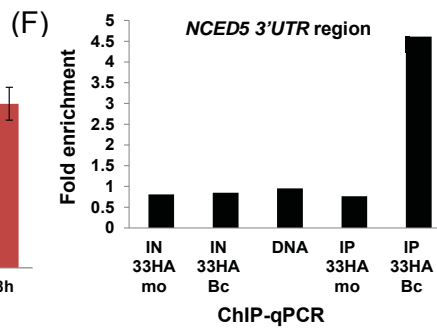
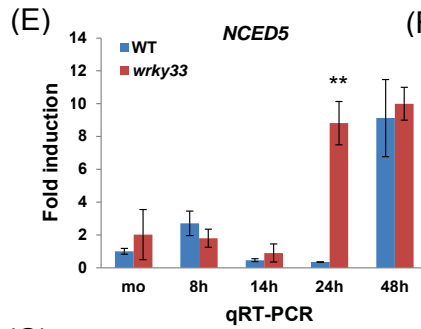
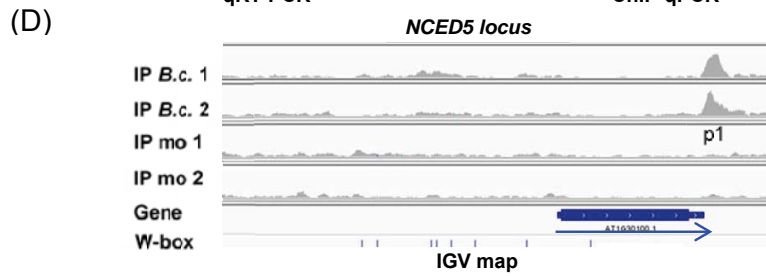
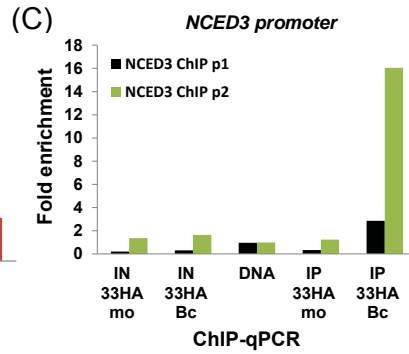
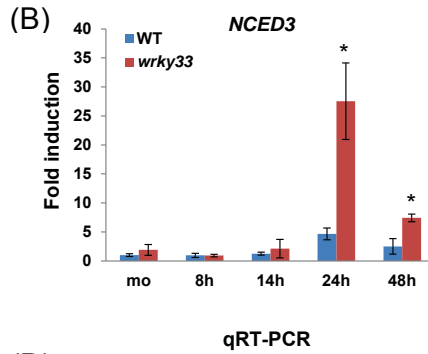
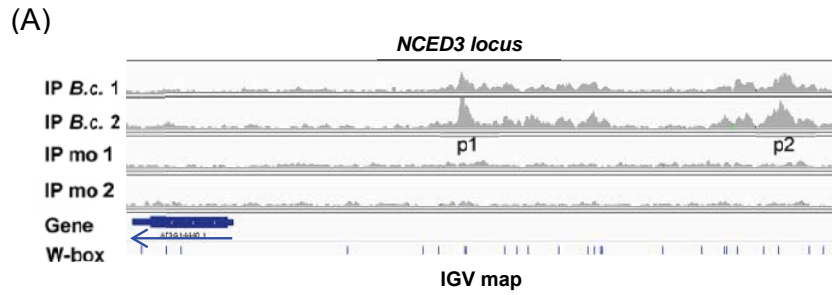
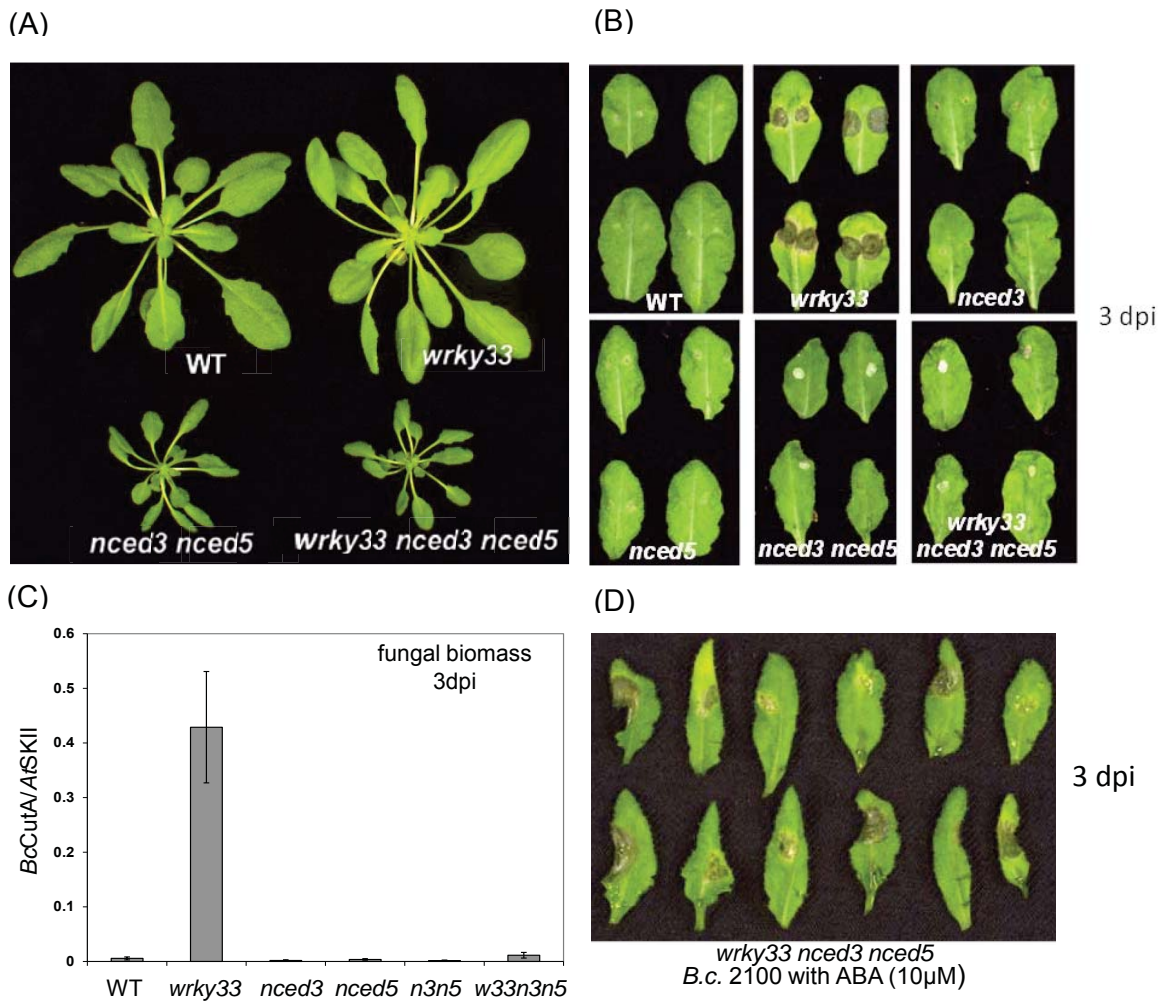


Figure 4



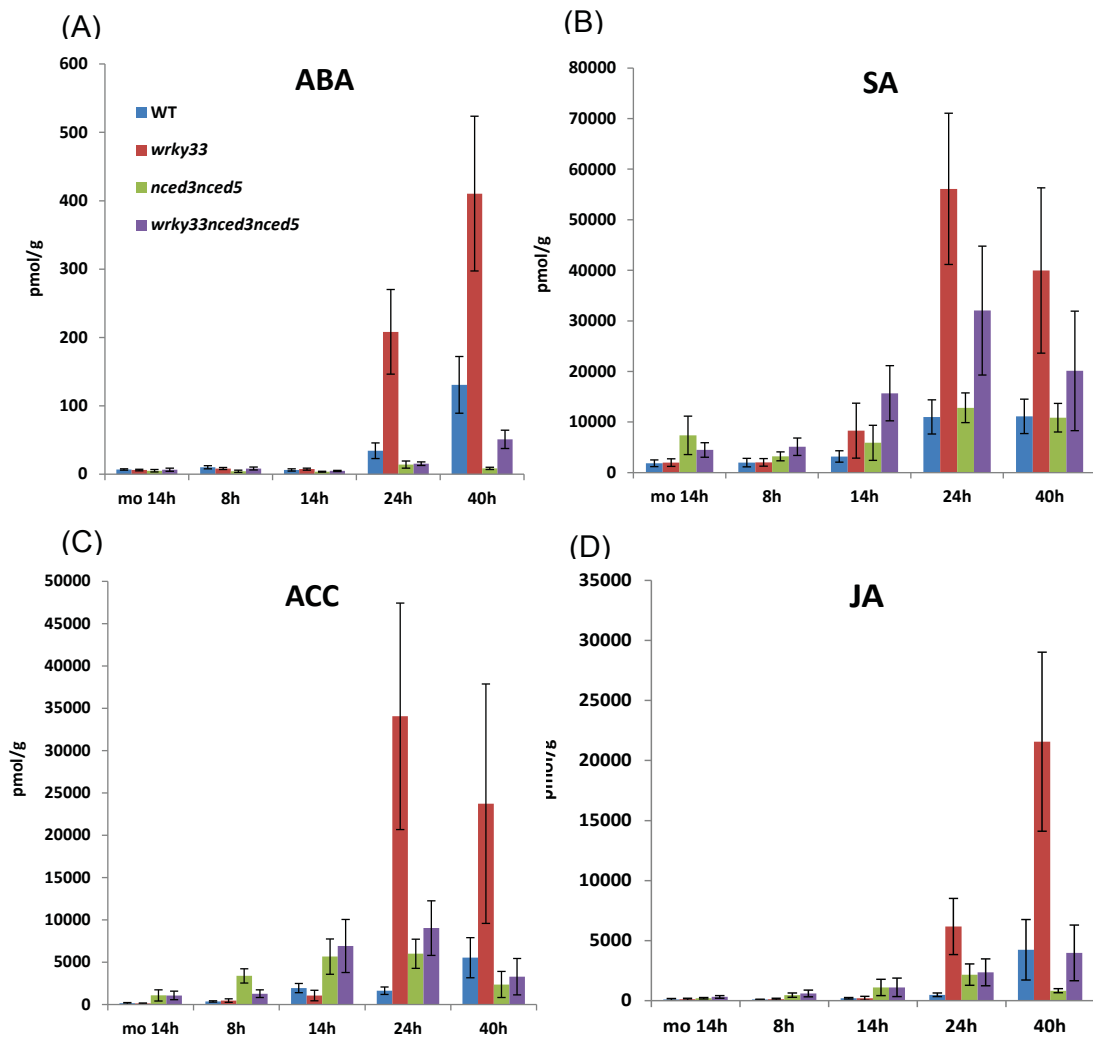


Figure 6

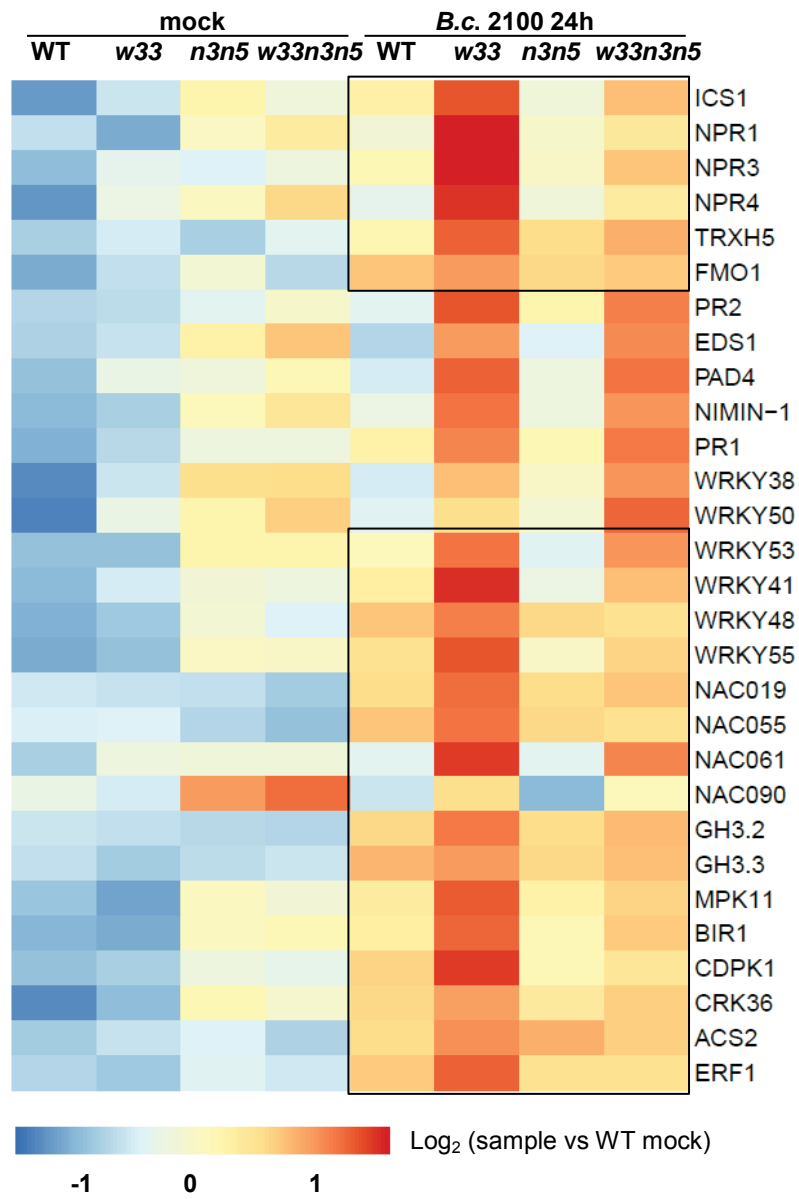


Figure 7

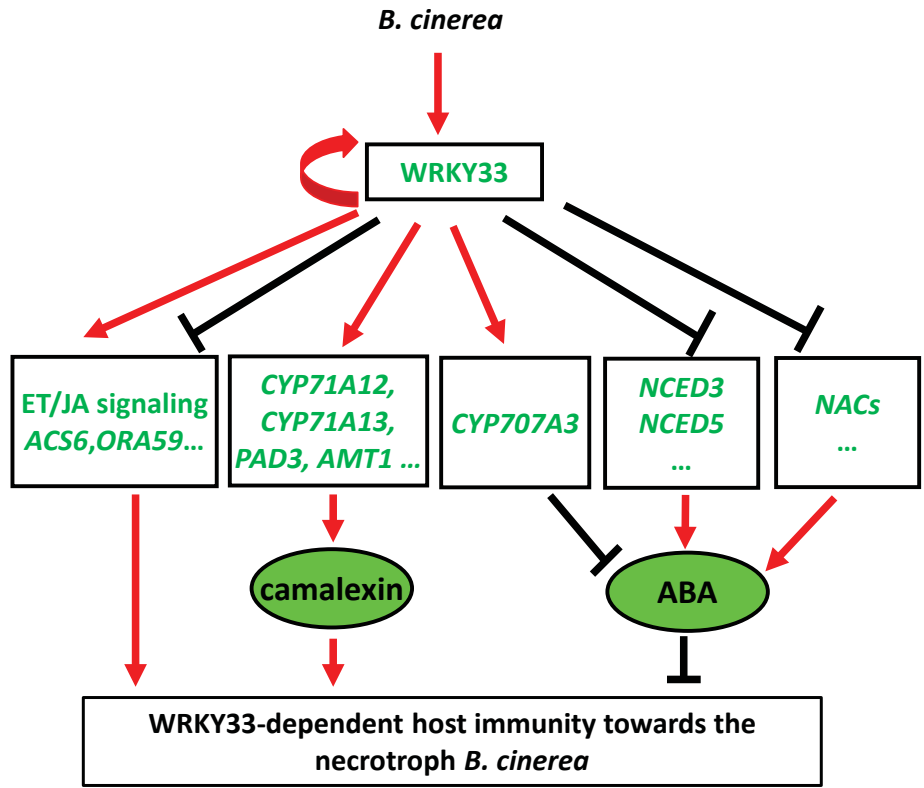


Figure 8